Brazilian Journal of Analytical Chemistry
Pre-publication – Accepted after peer review
doi: 10.30744/brjac.2179-3425.AR-46-2026

BrJAC

ARTICLE

Magnetic Molecularly Imprinted Polymer Covered with Polyethylene Glycol: A Restricted Access Material for Protein Exclusion

Rafael Rovatti Pupin*[1], Gustavo Claro Monteiro[1], Vanderlan da Silva Bolzani[1], María Isabel Pividori[2], Maria Del Pilar Taboada Sotomayor[1]

[1]*Instituto de Química, Universidade Estadual Paulista (UNESP). Araraquara, SP, 14800-060, Brazil*
[2]*Grup de Sensors i Biosensors, Departament de Química, Universitat Autònoma de Barcelona. Barcelona, 08193, Spain*

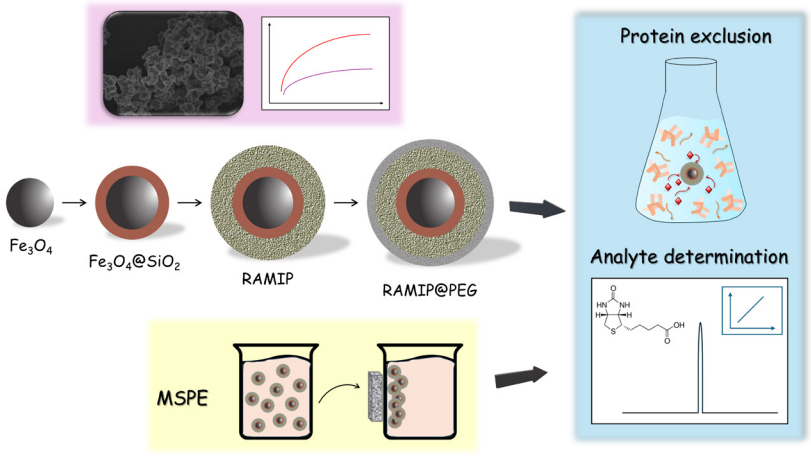

Restricted access molecularly imprinted polymers (RAMIPs) are a class of polymeric materials that exhibit high selectivity for analyte adsorption while possessing the ability to prevent the adsorption of macromolecules on their surface. In this work it is described the synthesis and characterization of a magnetic molecularly imprinted polymer (MMIP) selective to biotin covalently modified with polyethylene glycol (PEG) as restricted access agent. MMIP was initially modified with hydrophilic comonomers 2-hydroxyethyl methacrylate and glycerol dimethacrylate to insert free hydroxyl groups on the polymer surface and, in subsequent stage, through an esterification reaction, PEG was covalently linked to the surface. The materials obtained in each synthesis steps were characterized by different physicochemical techniques, until obtaining the molecularly imprinted polymer coated with PEG (RAMIP@PEG). In this proof-of-concept study, protein exclusion tests showed that the optimized polymer had an exclusion capacity in the range of 96 and 98% for the concentrations evaluated. Adsorption studies showed that the restricted access polymer bound to biotin, whose isotherm curves show a maximum adsorption (q_{max}), in the evaluated concentration range, of 3.2 mg g^{-1} for the imprinted polymer and 0.88 mg g^{-1} for the respective non-imprinted polymer. The results demonstrated that the synthesized polymer is an excellent adsorbent for biotin analysis and can efficiently exclude macromolecules.

Cite: Pupin, R. R.; Monteiro, G. C.; Bolzani, V. S.; Pividori, M. I.; Sotomayor, M. P. T. Magnetic Molecularly Imprinted Polymer Covered with Polyethylene Glycol: A Restricted Access Material for Protein Exclusion. *Braz. J. Anal. Chem.* (Forthcoming). https://doi.org/10.30744/brjac.2179-3425.AR-46-2026

Received: April 22, 2026; **Revised:** August 1, 2026; **Accepted:** August 18, 2026; **Published online:** September, 2026.

This article was submitted to the BrJAC Special Issue dedicated to Prof. Dr. Lauro Tatsuo Kubota.

Keywords: magnetic molecularly imprinted polymer, protein exclusion, restricted access material, magnetic solid-phase extraction, biotin

INTRODUCTION

Molecularly imprinted polymers (MIPs) are a class of materials known for their high selectivity to a target molecule due to the presence of selective binding cavities that are physically and chemically complementary to the analyte.[1] Different synthesis strategies can be adopted to obtain polymers with specific morphologies and properties, with the choice of MIP structure and production strategy mainly based on the desired analytical application.[2] MIPs can be used in the identification of low molecular weight analytes to macromolecules;[3] applied in the construction of sensors,[4] drug delivery systems,[5] sample preparation[6] and applications in the environmental field,[7] food analysis;[8] among numerous others.

Biotin (or vitamin B7) is a micronutrient that has a chemical structure composed of an imidazolidone ring fused with a tetrahydrothiophene ring and a valeric acid side chain is attached to the tetrahydrothiophene ring. Its structure features three asymmetric carbons, giving rise to eight stereoisomers and only d-(+)-biotin possesses biological activity; acting in cellular metabolism as an enzymatic cofactor, among several other roles.[9,10] One of the most notable and important characteristics of biotin is its high affinity for avidin (a tetrameric glycoprotein derived from egg white) or streptavidin (an avidin analogue derived from the bacterium *Streptomyces avidinii*). The biotin-avidin complex is considered one of the most specific and stable non-covalent interaction known ($K_d \sim 10^{-15}$ M). This high affinity allows these proteins and biotin to be a vital tool in biological applications and diagnostics.[11]

The valeric acid side chain of biotin can be chemically modified to incorporate various functional moieties, enabling its conjugation to different biomolecules such as nucleic acids, enzymes, antibodies, proteins or other.[12,13] Biotin-binding proteins, when conjugated to reporters such as enzymes, fluorophores or nanoparticles, allow the sensitive and specific detection and quantification of biotin and biotinylated targets.[14] The use of MIPs is emerging as an alternative to biological materials as recognition phase in analytical systems; and more specifically, MIPs for biotin have been successfully employed in biomimetic assays as substitutes for avidin/streptavidin.[14,15]

MIPs with different designs and methodologies have been developed to address limitations such as heterogeneous binding sites, slow binding kinetics, and template leakage; all of which directly impact the degree of selectivity and sensitivity of analyte recognition.[16,17] Another important factor to consider is the type of sample, since complex matrices (such as food, biological or environmental fluids) have a number of components that do not allow direct analysis and, moreover, compared to the concentration of these components, the concentration of the analyte is much lower, which makes analysis difficult.[18]

In this context, food and biological samples (such as urine, blood, etc.) contain macromolecules (proteins, lipids, carbohydrates, among others), and the use of MIP as a material for solid-phase extraction (SPE) ends up being limited since the macromolecules can adsorb on the surface of the polymer, blocking its selective cavities and consequently reducing its analytical performance.[19,20] One way to overcome this limitation was to modify the surface of polymers with functional groups or molecules that prevent the adsorption of macromolecules while the analyte is adsorbed selectively in the specific cavities. Restricted access materials (RAMs) achieve macromolecule exclusion based on physical separation by pore size and chemical separation by creating a hydrophilic barrier: the pore size allows only macromolecules to enter, while the chemical barrier prevents macromolecules from binding to the material's surface.[21]

RAM technique combined with MIPs has enabled the creation of molecularly imprinted polymers with restricted access (RAMIPs), which can act based on different modifications to their structures, the most commonly reported being modification with hydrophilic comonomers, comonomers that become hydrophilic after a reaction, and the combination of the use of hydrophilic comonomers and bovine serum albumin (BSA).[20,22]

Mendes et al.[23] developed a magnetic RAMIP for nicotine determination in biological samples. To exclude macromolecules, the polymer was modified after synthesis by recovering its surface with BSA and the

RAMIP showed a protein exclusion capacity of 99% compared to 79% for unmodified MIP. The proposed material presented good precision, recovery capacity and can be reused for at least 50 cycles without losing its nicotine extraction efficiency in human plasma.

Although highly efficient at excluding macromolecules, RAMIPs have some limitations such as significant nonspecific binding and a limited pH range for protein exclusion by electrostatic repulsion, given the type of technique used to obtain restricted access.[21,22] Almost all studies reported on the synthesis and evaluation of RAMIPs use hydrophilic comonomers and/or BSA coating as a restricted access strategy.

This work proposes the use of polyethylene glycol (PEG) as a restricted access agent for MIPs given the important properties that PEG presents. The process of conjugating PEG to nanoparticles via functional groups (a process known as PEGylation) by adsorption or grafting is advantageous given the properties of PEG such as electrical neutrality, spatial repulsion, and hydrophilicity.[24] PEG can be used as a blocking agent for the non-specific binding sites inherently formed in the MIP structure. A MIP grafted with a linear chain PEG has reduced binding of interfering molecules due to steric hindrance, in addition to increasing the material's biocompatibility, improving dispersibility and enhancing adjustable physicochemical properties.[25,26]

Given the need for highly efficient and selective materials with restricted access, this study reports the synthesis of a new biotin selective magnetic RAMIP coated with PEG (RAMIP@PEG) for use in protein exclusion. Morphological and physicochemical characterizations were performed to assess the properties of the obtained materials and to monitor the modifications. In this proof-of-concept study, the proposed polymers were evaluated for their protein exclusion capacity using BSA solutions as model and equilibrium and kinetic adsorption studies were conducted to evaluate the adsorption properties of the polymer by biotin, which showed that the proposed polymer exhibited high protein exclusion capacity while efficiently binding to biotin. Therefore, this work aims to contribute to the special issue in which it is included, with advances in the field of developing (bio)analytical materials and methodologies.

MATERIALS AND METHODS

Reagents and solutions

All reagents used were purchased in analytical grade. Ultrapure water was obtained from a Direct-Q 3UV Milli-Q water purification system (Millipore). Biotin, acrylic acid, ethylene glycol dimethacrylate (EGDMA) and 2,2'-azo-bis-2-methylpropionitrile (AIBN) were supplied by Sigma-Aldrich. 2-hydroxyethyl methacrylate (HEMA), glycerol dimethacrylate (GDMA), poly(ethylene glycol) bis(carboxymethyl) ether (PEG), bovine serum albumin (BSA) and thionyl chloride were purchased from Sigma-Aldrich. Biocytin and tetracycline were supplied by Sigma-Aldrich and succinimidyl-2-(biotinamido)ethyl-1,3-dithiopropionate (NHS-SS-biotin) by Thermo Scientific. Methanol was obtained from Panreac, glacial acetic acid and dichloromethane from Synth. Iron (II) chloride tetrahydrate, iron (III) chloride hexahydrate and 3-(trimethoxysilyl)propyl methacrylate (MPS) were purchased from Sigma-Aldrich; ammonium hydroxide, ethanol, and toluene were purchased from Synth and tetraethyl orthosilicate (TEOS) from Acrois.

All high-performance liquid chromatography (HPLC) measurements were performed using HPLC-grade methanol and acetonitrile, both from Panreac. For mobile phase optimization, phosphoric acid (Mallinckrodt) was used to prepare the acidified aqueous mobile phase.

Instrumental analysis

Materials characterization

Bruker Vertex 70 FT-IR spectrometer was used for Fourier transform infrared (FT-IR) measurements, with a HeNe laser source and DLaTGS detector, analyzing a range of 4000 to 400 cm^{-1}. The analysis was performed directly on the solid samples in attenuated total reflectance mode.

The morphology of the polymers was evaluated using a field emission scanning electron microscope (FEG-SEM) JEOL, JSM 6330F model. The materials were dispersed in isopropyl alcohol and placed in an ultrasonic bath for 10 minutes.

The porosity and surface area of the RAMIPs were evaluated by measuring N_2 sorption using the Micromeritics GEMINI VII instrument. The samples were pre-treated in vacuum for 3 h and degassed with helium at 250 ºC. The surface area was calculated according to the Brunauer–Emmett–Teller (BET) method, the pore volume calculated from the adsorption at P/P0 = 0.98 and the pore size by the Barrett-Joyner-Halenda (BJH) method.

The thermal stability of the materials was evaluated by thermal analysis using thermogravimetry (TG) and differential scanning calorimetry (TG-DSC). TG curves were obtained using a Mettler Toledo STARE TG-DSC system. A mixture of compressed air and N_2 at a flow rate of 50 mL min^{-1} was used as purge gas and the heating rate was 10 °C min^{-1} with 10.0 mg sample mass. DSC curves were obtained using a TA Instruments® Q10 DSC. The purge gas condition was the same as that used for TG, with a heating rate of 5 °C min^{-1} and 10.0 mg sample mass.

Vibrating sample magnetometry measurements for magnetic characterization were performed using the LakeShore VSM 7300 series equipment at the Bariloche Atomic Center, Magnetic Resonance Division, Argentina.

The determination of the materials' composition and analysis of the chemical bond structure was performed by X-ray photoelectron spectroscopy (XPS). A UNI-SPECS UHV System spectrometer was used with a pressure lower than 5×10^{-7} Pa. The Mg Kα line (hv = 1253.6 eV) was used as the ionization source, and the analyzer's pass energy was adjusted to 10 eV. The atomic percentage composition of the surface layer (<5 nm) was determined by the relative proportions of the spectral areas, and the binding energy scale of the spectra was corrected using the hydrocarbon component fixed at 285.0 eV.

Solid-state nuclear magnetic resonance (NMR) analysis yielded ^{1}H and ^{13}C spectra using a Bruker Avance III 400WB HD (9.4 T) spectrometer with a 4 mm CP/MAS DVT triple resonance low gamma probe, with a frequency range from ^{39}K to ^{2}H, operating in a temperature range from −120 ºC to 150 ºC; and a CP/MAS DVT triple/double resonance probe with double resonance BB/^{1}H, with a frequency range (BB) from ^{15}N to ^{31}P.

Analytical measurements

For pH measurements a Gehaka Digital pH meter model PG 2000 was employed. Spectrophotometric measurements were performed on a Bel Photonics UV-M 51 UV-Vis spectrophotometer, controlled by the UV Professional 2 software. All measurements were performed in a 1.0 cm optical path quartz cuvette and wavelength scanning in the range of 200 to 350 nm.

High-performance liquid chromatography (HPLC) analyses were performed using a Shimadzu chromatograph, model 20A with a UV-Vis detector model SPD-20A, SIL-20A autosampler and DGU-20A5 degasser, coupled to a microcomputer. The stationary phase used was a Shim-Pack VP-ODS reverse-phase column 4.6 µm (particle size) 12 nm (pore diameter), 250 mm long x 4.60 mm internal diameter. The mobile phase was prepared by mixing an aqueous solution containing 0.1% H_3PO_4 with acetonitrile (ACN) in an 80:20 (v/v) ratio, at a flow rate of 1.0 mL min^{-1}. Detection was performed using a wavelength of 210 nm and a sample injection volume of 10 µL.

Synthesis and modification of materials

Magnetite nanoparticles and biotin magnetic MIP

The synthesis of magnetite (Fe_3O_4) nanoparticles and its modifications with TEOS and MPS were conducted according to method reported in three different steps.[27] In summary, co-precipitation of 0.01 mmol of Fe^{2+} and 0.02 mmol of Fe^{3+} was performed in basic medium: $FeCl_2{\cdot}4H_2O$ and $FeCl_3{\cdot}6H_2O$ salts were dissolved in 80.0 mL of ultrapure water heated to 80 °C, then 10.0 mL of NH_4OH was added dropwise. The black precipitate (Fe_3O_4) was washed several times with distilled water until neutral pH and dried for 24 h. Subsequently, for silanization of the nanoparticles, 0.8 mL of TEOS was added to 500 mg of nanoparticles dispersed in 80.0 mL of ethanol and 8.0 mL of ultrapure water. The mixture reacted for 12 h at room temperature and was subsequently washed with water until neutral pH and dried for 24 h. In the final step, for the functionalization of the nanoparticles with the insertion of a methacrylic group, 250 mg of

the nanoparticles were dispersed in 50.0 mL of anhydrous toluene and 5.0 mL of MPS under mechanical stirring for 12 h under a flow of nitrogen. The resulting product was washed with toluene, four times with ethanol, extensively with water and dried for 24 h.

Magnetic MIP (MMIP) for biotin was obtained according to the following: biotin (0.2 mmol), acrylic acid (0.08 mmol) and 40 mL of ethanol were mixed for 12 h at 25 °C. Next, 200 mg of modified magnetite nanoparticles were added, and the system was kept under constant stirring for 2 h. Finally, 4.0 mmol of EGDMA and 0.05 mmol of AIBN were added to the mixture, the reaction system was sealed and N_2 was continuously purged into the solution. The system was heated to 60 °C for 5 h and after the synthesis was complete, the polymer was washed in a Soxhlet system with methanol/water to remove biotin and excess reagents.[28] Similarly to MMIP, a magnetic non-imprinted polymer (MNIP) was synthesized as a control material and its synthesis is identical to that of MMIP; however, there is no addition of the analyte.

Magnetic MIP with restricted access (RAMIP) and its modification with PEG (RAMIP@PEG)

A mixture of two different hydrophilic comonomers, HEMA and GDMA was used to make MMIP a restricted-access material and the synthesis procedure adopted was exactly the same as for MMIP, evaluating five different times of insertion of the comonomers in separated syntheses, as shown in Table I (considering the start time of the synthesis as the moment after the addition of the radical initiator).

Table I. Parameters evaluated for RAMIP: proportion and time of addition of hydrophilic comonomers

EGDMA:HEMA:GDMA ratio (mmol)	Time for adding comonomers after the synthesis started (min)
1 : 0.5 : 0.06 1: 1 : 0.1 1: 2 : 0.25	0* (RAMIP 1) 45 (RAMIP 2) 60 (RAMIP 3) 90 (RAMIP 4) 120 (RAMIP 5)

*Before initiating polymerization, at the same time as the other reagents.

By maintaining a constant analyte:functional monomer:structural monomer ratio (1:4:20, respectively), the best ratio of hydrophilic comonomers in the synthesis was evaluated based on the ratio of the structural monomer EGDMA (Table I). A mixture of HEMA and GDMA, in the proportions described above, was prepared separately in the same synthesis solvent and continuously purged with N_2. The syntheses were performed separately, maintaining constant the reactant proportions while varying the timing of comonomer addition; thus, a different RAMIP polymer was synthesized for each time that was evaluated.

The experimental procedure for the synthesis of RAMIP polymers was performed following these steps: i) MMIP synthesis was initiated as previously described, and after adding AIBN initiator and sealing the system, timing was started for the addition of the mixture; ii) after the specified time (Table I), the HEMA/GDMA mixture was added dropwise; iii) the system was kept sealed and under continuous N_2 flow until the end of the polymerization (5 h of reaction).

The polymers were washed with solvents at room temperature, under mechanical agitation, using a methanol/water mixture, and the solutions were monitored by UV-Vis spectrophotometry.

Considering the best conditions 1:1:0.1 mmol EGDMA:HEMA:GDMA and 45 min for comonomers addition, modification with PEG was carried out, whose experimental procedure was based on a general esterification reaction;[29] as described: 100.0 mg of RAMIP interacted with 5.0 mL of PEG solution (prepared in dichloromethane, which was previously treated with calcium hydride and distilled before use). Then, the system temperature was adjusted to 0 ºC and, drop by drop and with magnetic stirring, 0.3 mL of thionyl

chloride was added. The reaction system was maintained under these conditions for 5 min and then heated to 30 ºC for 12 h. The final product (RAMIP@PEG) was washed three times with dichloromethane (using a rotary evaporator) and exhaustively with distilled water. Subsequently, it was placed to dry under vacuum. As control material, a non-imprinted polymers with restricted access (RANIP@PEG) were synthesized using the same procedure without the addition of biotin.

In order to optimize the material and evaluate the effect of the proportion of PEG that was covalently bonded to the MIP surface, while keeping the RAMIP mass constant, syntheses were performed for the following amounts of PEG in mmol: 0.025; 0.0625; 0.0937; 0.125; 0.25 and 0.50.

Analytical performance of the polymers

All assays were performed using the polymers in magnetic solid-phase extraction (MSPE) technique, and several parameters were evaluated in the MSPE optimization.

Protein exclusion assay

10.0 mg of each RAMIP@PEG was weighed into plastic tubes and it was added 1.0 mL of different concentrations of BSA solution (0.1; 0.5 and 1.0% m/v) prepared in 50 mmol L^{-1} phosphate buffer pH 6.0. The BSA solutions and polymers interacted for 10 min under gentle mechanical stirring. After this time, the magnetic polymers were separated using an external neodymium magnet and the solution analyzed by spectrophotometry in the ultraviolet-visible (UV-Vis) region. The amount of BSA excluded was calculated by the difference between the total amount and the residual amount detected in the supernatant.

RAMIP@PEG adsorption studies

For all adsorption experiments described below, after the end of the interaction time under constant agitation, the polymers were separated from the solution by applying a magnetic field (using an external neodymium magnet) and the supernatants were filtered through 0.45 µm hydrophilic polytetrafluoroethylene (PTFE) filters and evaluated by HPLC. The amount of biotin adsorbed was calculated by the difference between the total amount and the residual amount detected in the supernatant (Supplementary Material, Equation S1). According to the difference in biotin concentration before and after adsorption, the adsorption capacity Q (mg g^{-1}) of the polymers was calculated using Equation (1):

$$Q_e = \frac{(C_i - C_e) \times V}{m} \qquad (1)$$

where Q_e (in mg g^{-1}) is the amount of biotin (mg) adsorbed per gram of the polymer in equilibrium; C_i is the initial and C_e is the equilibrium concentration (mg L^{-1}) of biotin; m is the mass (g) of polymer and V is the volume (L) of solution.

To optimize the efficiency of RAMIP@PEG for biotin identification, adsorption parameters were evaluated as described following. To evaluate the rebinding solvent, 10.0 mg of polymer interacted with 5.0 mL of a 20.0 mg L^{-1} biotin solution prepared in different solvents (water, methanol, ethanol, acetonitrile, and mixtures of water and organic solvents) for 120 min.

To evaluate the best amount of mass for analyses with RAMIP@PEG, an adsorbent dosage study was conducted in which different masses of polymer, from 5.0 to 50.0 mg, and these masses interacted with an initial concentration of 50.0 mg L^{-1} biotin solution prepared in methanol.

After defining the best polymer mass for the studies, a kinetic study was evaluated: 5.0 mg of RAMIP@PEG interacted with 50.0 mg L^{-1} of biotin solution prepared in methanol for different times; in a range from 10 to 300 min.

To construct the adsorption isotherm curves, 5.0 mg of polymer interacted for 90 min with different concentrations of biotin (from 5.0 to 100.0 mg L^{-1}) prepared in methanol.

Selectivity test

Biocytin, NHS-SS-Biotin and tetracycline were used to test the selectivity of RAMIP@PEG for biotin and RANIP@PEG as control. The experiment was performed under optimized conditions: 5.0 mg of the polymers were dispersed in 5.0 mL of methanol solutions for each of the interferents (80 mg L^{-1}) evaluated separately. After 90 min of interaction under mechanical agitation, the polymers were separated using an external magnet, the supernatants were filtered through a 0.45 µm PTFE filter and analyzed by HPLC.

The distribution coefficient (K_d) and imprinting factor (*IF*) were calculated, respectively, according to Equations (2) and (3) [28,30] as follows:

$$K_d = \frac{(C_i - C_e)}{C_e} \times \frac{V}{m} \quad (2)$$

where K_d is the distribution coefficient (L g^{-1}), C_i is the initial and C_e is the equilibrium concentration (mg L^{-1}) of the studied molecule; m is the mass (g) of polymer and V is the volume (L) of solution.

$$IF = \frac{K_{d-MIP}}{K_{d-NIP}} \quad (3)$$

where $K_{d\text{-}MIP}$ and $K_{d\text{-}NIP}$ are, respectively, the distribution coefficients of the imprinted (RAMIP@PEG) and non-imprinted (RANIP@PEG) polymers.

RESULTS AND DISCUSSION

Synthesis

The synthesis of RAMIP was carried out by adding hydrophilic comonomers to the MMIP synthesis, with the aim of making MMIP surface polar. The technique involved initiating the polymer synthesis of the MMIP, in which the functional monomer and cross-linker polymerized around the biotin molecule; after a certain period, the comonomer mixture was added, and the reaction proceeded for a few more hours until completion. Because HEMA and GDMA have free hydroxyl groups, due to repulsion with the hydrophobic polymer chain, these polar groups are oriented outwards from the polymer structure, appearing free on the surface, as proposed in Figure S1 (Supplementary Material). This method of grafting hydroxyl groups to obtain the hydrophilic layer is one of the principal methods in obtaining RAMIP particles.[31]

The RAMIPs were washed with solvents at room temperature and using a lower proportion of acid compared to the MMIP cleaning, since common conditions (such as acid medium and high temperature) favor the hydrolysis of the hydroxyl groups on the surface.

To evaluate the RAMIP formed, when testing different EGDMA:HEMA:GDMA ratios (Table I), it was observed that for the 1:1:0.1 mmol ratio, biotin was able to bind satisfactorily to RAMIP, whereas for the other two ratios evaluated, no retention of biotin has occurred. Then, PEG was immobilized through an esterification reaction with the hydroxyl group present on the RAMIP surface. Figure 1 illustrates the (unbalanced) steps of the RAMIP coating reactions, as described in the experimental procedure: first, the PEG dicarboxylic acid is activated, forming a chlorinated derivative; subsequently, the nucleophilic reaction of the hydroxyl group (of HEMA on the MMIP surface) with the chlorinated derivative of PEG occurs. The proposed mechanisms of reactions can be seen in Figures S2 and S3.

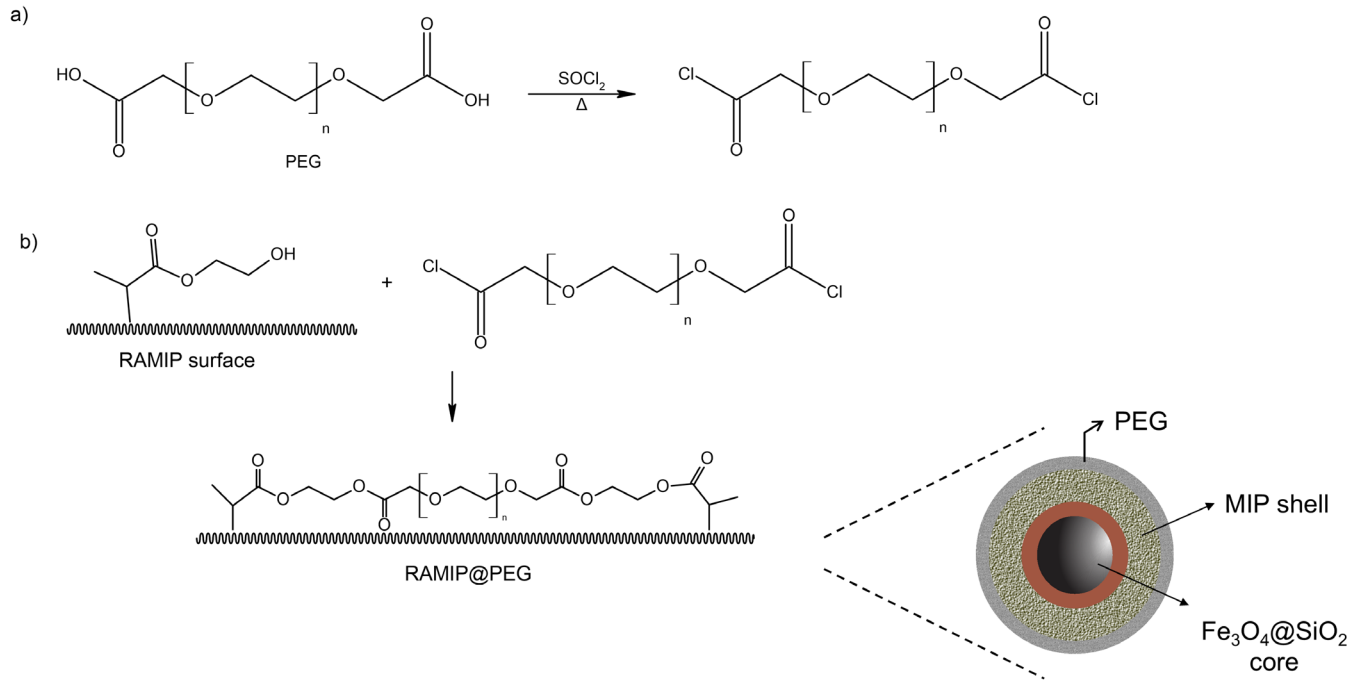

Figure 1. Reaction steps for the synthesis of RAMIP@PEG, with a) formation of the chlorinated PEG derivative and b) covalent immobilization of PEG on the RAMIP surface.

Polymers characterizations

The synthesis of nanoparticles and MMIP for biotin is already well established;[28] therefore, the characterizations were focused on the restricted access materials; while MMIP was evaluated as comparison standard for all modifications performed.

FT-IR measurements (Figure 2) were applied to confirm the presence of free hydroxyl groups on the RAMIP surface. The comonomer mixture was added at different times after the polymer's synthesis started, grafting hydroxyl groups in the polymer structure since a bond occurs between the vinyl group of monomers and the growing polymer chain. All syntheses were evaluated according to the insertion time of the hydrophilic comonomers HEMA and GDMA (Table I).

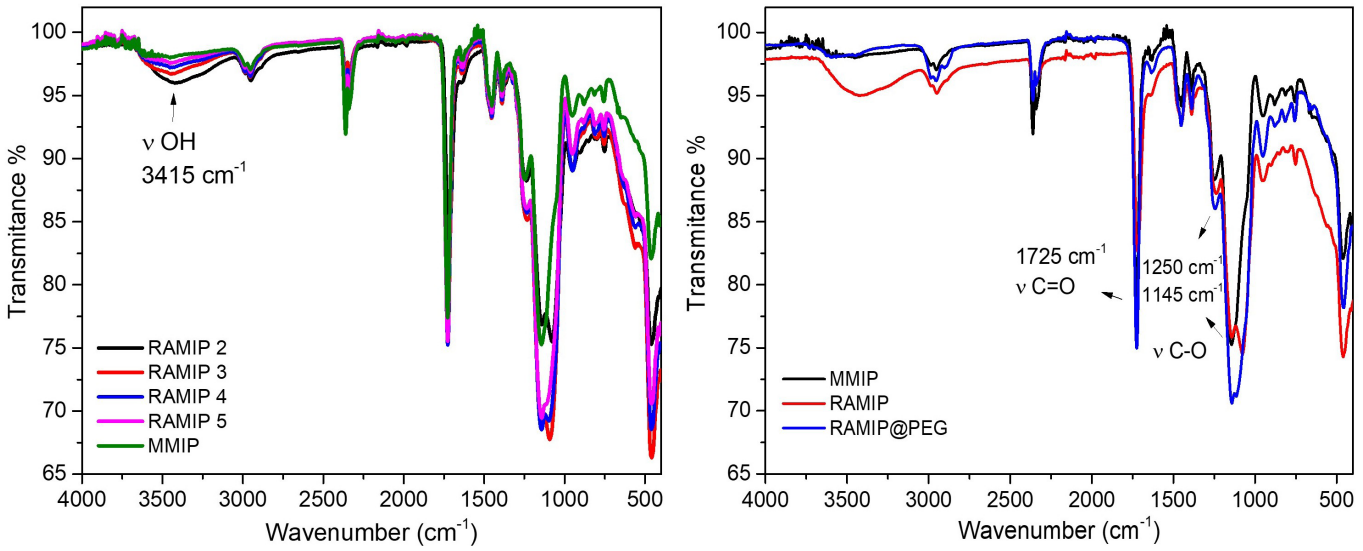

Figure 2. FT-IR spectra with assignment of the main bands for the various synthesized RAMIP and among the different polymers MMIP, RAMIP, and RAMIP@PEG.

RAMIP 1 is not shown in FT-IR spectra because this synthesis did not occur; the polymer was not formed possibly because the comonomers were added at the same time as all the other reagents. Since the free radical polymerization mechanism does not differentiate double bonds, radicals of EGDMA, HEMA and GDMA were formed and crosslinked in a disordered manner, preventing the construction of the polymer chain. An excess of free hydroxyl groups prior to the start of the reaction can act as functional monomers and hinder the linking of EGDMA radicals to form the main polymer structure. The functional monomer: crosslinker ratio significantly impacts on the physical characteristics as the polymer rigidity and other properties.[2]

In Figure 2, the syntheses 2 to 5 show the presence of OH stretching (3415 cm^{-1}), which decreases in intensity as the comonomers insertion time increases. Based on this, a possible conclusion is that the degree of comonomer grafting varied with the insertion time, likely depending on the stage of the main polymer macrochain's formation. Free-radical polymerization comprises three stages: initiation, propagation, and termination. During the propagation stage, the macromolecular polymer chain is formed through the successive addition of monomers to a growing macroradical, resulting in high molecular weight polymer chains.[32] At shorter times, a greater number of radicals are available during the propagation stage, allowing for a higher level of comonomer grafting into the growing macroradical polymer chain. At longer times, the polymer macroradical, and the resulting polymer macrochain, is much more highly structured; consequently, there are fewer radical sites available for comonomer insertion, leading to a lower degree of functionalization.

Since synthesis 2 showed greater hydroxyl signal, this RAMIP was chosen to perform the subsequent modifications with PEG. Using infrared spectroscopy, it was not possible to evaluate the PEG coating, since only the carbonyl (1725 cm^{-1}) and C-O (1145 cm^{-1}) stretching bands were observed, characteristic of the major EGDMA composition in MIP polymeric structure.[33,34]

All synthesized polymers were analyzed by SEM to observe their morphology, distribution, and surface characteristics. According to Figure 3, it is possible to observe that the particles obtained for MMIP and RAMIP have a spherical and uniform shape, in addition to being slightly agglomerated. Figure 3c and Figure 3d shows RAMIP@PEG containing different proportions of PEG used in the synthesis, and it is not possible to verify a difference in the surface or morphology of the polymer particles after modification with smaller or larger amounts of PEG.

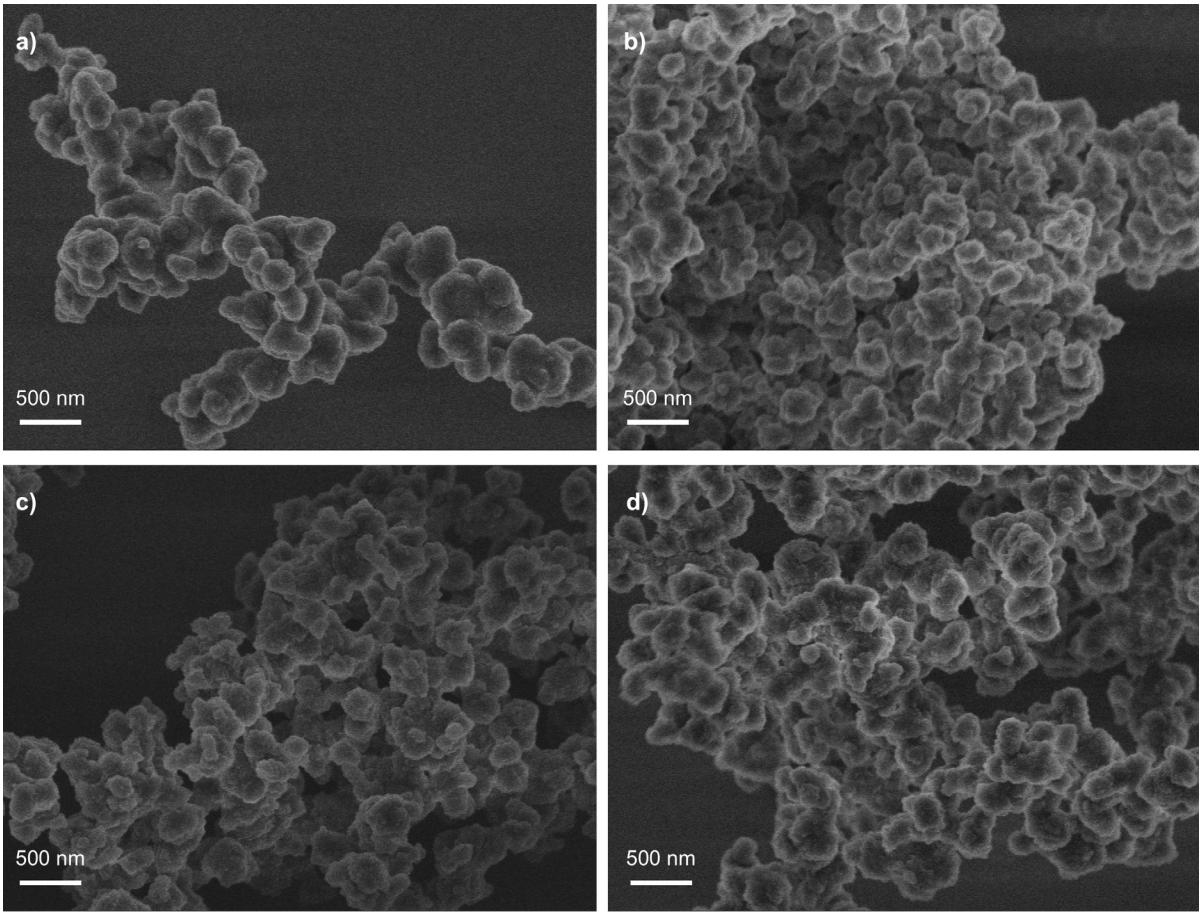

Figure 3. SEM images (magnification of 25000x) of: a) MMIP, b) RAMIP, c) RAMIP@PEG containing 0.0625 mmol of PEG and d) RAMIP@PEG containing 0.25 mmol of PEG.

The particle size varied according to its composition: 0.19 ± 0.03 μm for MMIP, 0.19 ± 0.02 μm for RAMIP, 0.20 ± 0.07 μm for 0.0625 mmol of PEG and 0.23 ± 0.02 μm for 0.25 mmol of PEG. Since the RAMIP modification is only the insertion of functional groups, the average particle size was close to that of MMIP. For the PEG modification, it was observed that the larger the amount of PEG used, the particle size was slightly larger, indicating a coating with a thicker layer.

XPS technique was performed to analyze the surface chemical composition of the different synthesized polymers. From the XPS spectra obtained (Figure 4), the binding energy and atomic percentage values (Table II) show differences in the amount of carbon and oxygen, making it possible to distinguish MMIP, RAMIP, and RAMIP@PEG.

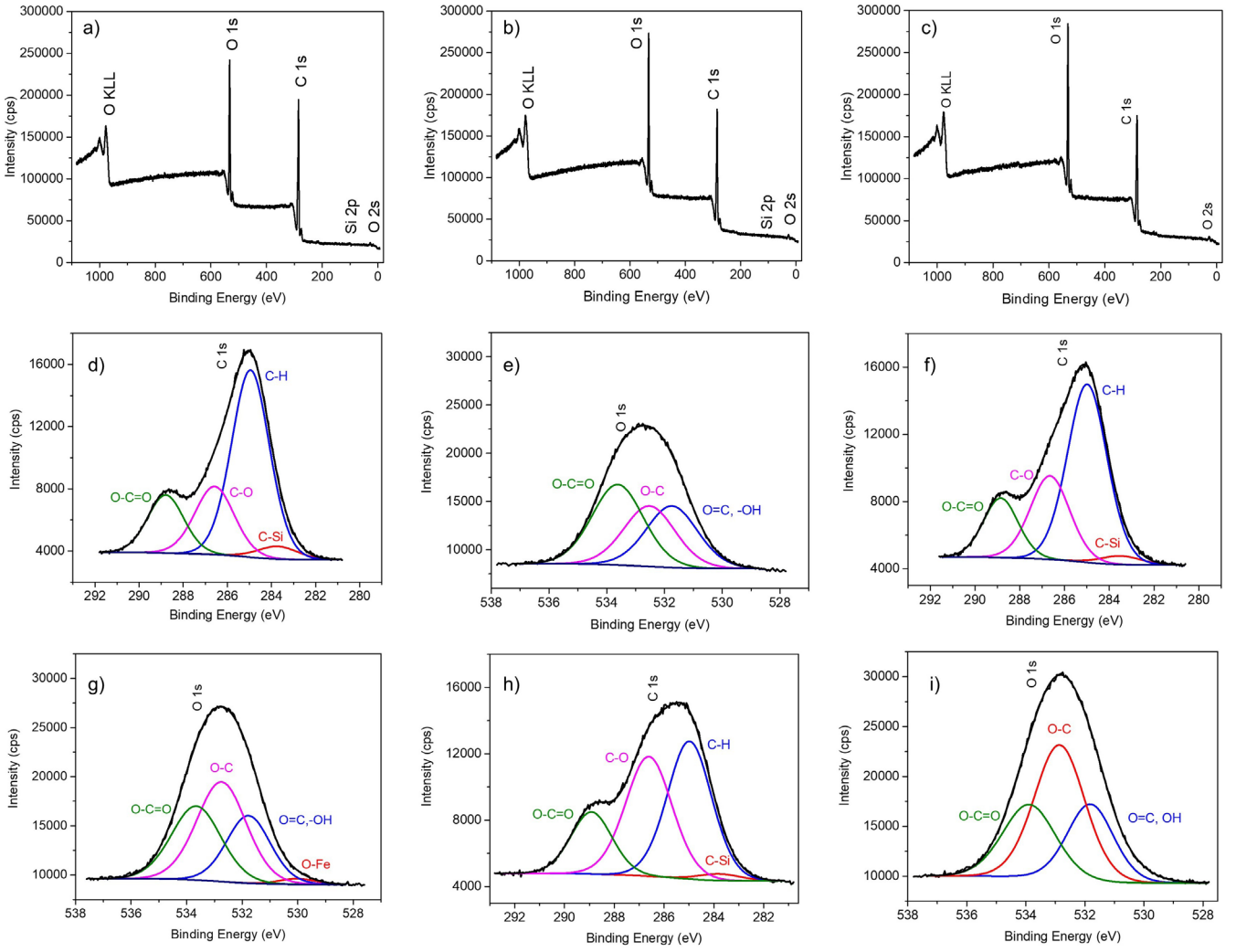

Figure 4. XPS spectra for a) MMIP; b) RAMIP; c) RAMIP@PEG; d) C 1s spectra for MMIP; e) O 1s spectra for MMIP; f) C 1s spectra for RAMIP; g) O 1s spectra for RAMIP; h) C 1s spectra for RAMIP@PEG and i) O 1s spectra for RAMIP@PEG.

Table II. Binding energy (B.E.) and atomic percentage (% At.) obtained from XPS spectra of the components present in the different polymers

Material	C 1s		O 1s		Si 2p	
	B.E (e.V)	% At.	B.E (e.V)	% At.	B.E (e.V)	% At.
MMIP	285.0	74.7	532.7	24.5	100.7	0.80
RAMIP	285.3	71.2	532.3	28.6	103.5	0.25
RAMIP@PEG	285.0	70.2	532.3	29.7	102.7	0.07

Analyzing the spectra for the different materials (Figure 4.a,b,c), Fe peak is not observed, only C and O signals, indicating complete coverage by the magnetic nanoparticles.[35] For PEG modification, the Si signal is also absent, possibly due to the increased thickness of the material layer resulting from the PEG

coating. The Immobilization of hydroxyl groups occurred on the surface of RAMIP, since, when comparing this polymer to MMIP, the percentage of oxygen present increased and there was an increase in carbon bond energy. Furthermore, polymerization reactions of MIP on the modified nanoparticles (Fe_3O_4@SiO_2) are effective and show great homogeneity, since the percentage of Si present (main component of the nanoparticle modification with TEOS) is at most 0.8%.

The C 1 s spectrum for MMIP (Figure 4.d) shows four components at 283.7 ev, 284.9 eV, 286.6 eV and 288.8 eV, which correspond respectively to C–Si, C–H, C–O, and O–C=O bonds. The O 1 s spectrum (Figure 4.e) for MMIP three components at 531.7 ev, 532.5 eV and 533.6 eV, which correspond to O=C, O–C, C–O, and O–C=O bonds, respectively. These characteristics are consistent with the structure of the momomers that compose the polymer chain.[35,36] The same bonds are observed in RAMIP and RAMIP@PEG, given their similar composition; and small variations in binding energy values are observed, possibly due to the structural differences.

For RAMIP@PEG, the presence of PEG as modifier was monitored by the percentage intensity of C–O bonds present in the polymer; resulting from the PEG immobilization reaction that was carried out through an esterification between the hydroxyl group of RAMIP and the activated acid PEG (Figure 1), forming an ester. Therefore, the amount of hydroxyl groups and ester bonds was monitored, comparing RAMIP and RAMIP@PEG.

By deconvolution of the photoelectron spectra for O 1s and C 1s for RAMIP@PEG, in Figure 4.h and Figure 4.i, respectively, the percentages of chemical bonds present were found by calculating the area of interest. Comparing with RAMIP, it was observed that the percentage of ester bonds (O–C=O) increased from 16.2% in RAMIP to 17.6% in RAMIP@PEG; while the percentage of hydroxyl groups decreased, respectively, from 25.14% to 24.1% when modified with PEG. Furthermore, there was an increase in O–C bonds from 42.0% in RAMIP to 45.9% in RAMIP@PEG. Therefore, it is possible to conclude that the immobilization and coating reaction of PEG on the RAMIP surface was successfully carried out.

The magnetization study, shown in Figure S4.a, demonstrated a decrease in the magnetization value of the MMIP as successive modifications are made. It is important to note that, given the superparamagnetic nature of Fe_3O_4 nanoparticles, even after several modifications, they continue to respond very satisfactorily to the application of an external magnetic field. Evaluating the influence of the amount of immobilized PEG, for larger proportions, such as 0.500 mmol, for example, the polymer completely loses its magnetization (a value found around 0.1 emu g^{-1}); since the excess PEG covers the entire surface of the RAMIP. Experimentally, the magnetic field of the neodymium magnet did not attract the particles; therefore, the use of smaller amount of PEG proved to be a critical factor in optimizing the material.

As shown in Figure S4.b, the thermal stability analysis of the materials allowed to calculate with good precision the mass of PEG deposited. The materials exhibit loss of adsorbed water in their structure up to 100 °C, PEG exhibits thermal stability up to a temperature of 175 °C, and RAMIP showed greater stability (without significant mass loss) than the RAMIP@PEG magnet, whose decomposition of the polymeric matrix started in the temperatures of 310 °C and 255 °C, respectively.[37]

PEG was immobilized since MIP@PEG showed a greater mass loss than the RAMIP, possibly leaving as residue the iron oxides resulting from the decomposition of magnetite, that remains due to its high melting point, while the polymers and modifying agents are organic components that are completely decomposed in the process within the evaluated temperature range.[38] Furthermore, the mass loss of RAMIP@PEG is proportional to the amount of PEG immobilized. With an increase in the proportion of immobilized PEG, there is a greater mass loss; and, when compared with RAMIP, and since PEG decomposes completely, it is possible to conclude that the decomposed mass refers to PEG. Thus, based on the difference in mass of the residues (comparing MMIP and RAMIP@PEG), it is possible to conclude that between 1.8% PEG (for 0.0625 mmol PEG) and 12.4% PEG (for 0.500 mmol PEG) were immobilized.

NMR analysis of the solid polymers (Figure S5) allowed to track changes in the chemical environment (both ^{1}H and ^{13}C) due to modification with hydrophilic comonomers and PEG. For signal assignment, the structures of the polymers and modifiers, which are known, were considered. However, since they are second-order spectra, it was not possible to perform the integration or calculation of the coupling constant.

The RAMIP shows low-intensity signals with chemical shifts typical of hydrocarbons, all in high field (Figure S5.a). At 0.21 ppm, the signal with the smallest chemical shift is observed, which can be attributed to the hydroxyl groups of the pro-hydrophilic comonomers, used in the same proportion as the structural monomer. At 1.44 ppm, there is a signal from the hydrogens corresponding to the methyl group. The signal at 1.37 ppm is attributed to the methylene groups. It was also possible to analyze the lower intensity signals, referring to the hydrogens of the esters (a functional group present that is repeated throughout the polymeric unit). At 2.1 ppm, the signal referring to the α hydrogens is observed, which are deshielded by the anisotropic effect of the carbonyl group. And from 4.12 to 5.43 ppm, a broad and undefined signal is observed, corresponding to the hydrogens of the carbon bonded to oxygen by a single bond. They exhibit deshielding due to the electronegativity effect.

For RAMIP@PEG (Figure S5.b), an intense signal is observed that splits, forming a false double doublet with a roof effect, which indicates that there is coupling between the protons involved in the signal – in the high field of RAMIP and the low field of PEG. Analyzing the spectrum, a hydrogen signal from the methyl group would be expected, a double double doublet (corresponding to $[O–CH_2–CH_2]_n$), and yet the signals mix, forming a false double doublet; being a second-order spectrum. The unfolding and roof effect can be attributed to the symmetry of the PEG molecule and due to the different chemical environments of the molecules in contact with the polymer surface.

Evaluating ^{13}C spectrum for RAMIP (Figure S5.c), from 13 to 30 ppm there is a broad signal corresponding to the CH_2 and CH_3 bonds. At 46.17 ppm a thinner and more intense signal corresponding to the C–O bond is observed. Finally, at 177.92 ppm the signal corresponding to the carbonyl (C=O) is visualized; the carbon being the most unshielded due to the anisotropic effect.

Also in the carbonyl region, as shown in Figure S5.d for the RAMIP@PEG spectrum, it was observed the appearance of a signal at 171.70 ppm; this signal can be attributed to the esterification reaction with PEG. Since the reaction occurs on the surface using different functional groups (plus the linear chain of PEG), the ester bonds formed are in a different chemical environment from the carbonyl group of the main polymer structure (which comes from EGDMA); therefore, it is possible to differentiate the carbonyl group of PEG from the carbonyl group of EGDMA.

The results of BET analysis comparing all synthesized materials are displayed in Table III. There was an increase in surface area due to the formation of a new polymeric layer around RAMIP that corresponds to PEG, and yet the average pore volume remained basically constant: 0.10 $cm^3\ g^{-1}$ for RAMIP with an average of 0.129 ± 0.004 $cm^3\ g^{-1}$ for RAMIP@PEG, considering the three different proportions of PEG evaluated. The reduction in the surface area of these two materials compared to the MMIP, as well as the decrease in average pore size, likely results from the immobilization of functional groups and the chemical bonding of PEG coating the surface; this behavior is observed when successive modifications using different compounds are performed on the MMIP surface.[39] Possibly, the limiting factor for the amount of PEG immobilized is due to the number of hydroxyl groups available on the RAMIP surface. The average pore size for MMIP e RAMIP@PEG is in a range between 2 and 50 nm, and they are classified as mesopores according to IUPAC recommendations.[40]

Table III. Porosity results obtained from BET isotherm for MMIP samples and the modifications with different PEG concentrations

Material	Superficial area ($m^2\ g^{-1}$)	Average pore volume ($cm^3\ g^{-1}$)	Average pore size (nm)
MMIP	62.2	0.0832	11.3
RAMIP	20.0	0.0803	8.72
RAMIP@PEG (0.0625 mmol PEG)	42.0	0.131	5.25

(continued on next page)

Table III. Porosity results obtained from BET isotherm for MMIP samples and the modifications with different PEG concentrations (continued)

Material	Superficial area ($m^2\ g^{-1}$)	Average pore volume ($cm^3\ g^{-1}$)	Average pore size (nm)
RAMIP@PEG (0.125 mmol PEG)	46.8	0,124	5.71
RAMIP@PEG (0.500 mmol PEG)	39.0	0,132	5.04

Protein exclusion assays

To evaluate the protein exclusion capacity of a restricted access MIP, the material is dispersed in a standard protein solution for a period, and this assay aims to assess the polymer's ability to adsorb or repel macromolecules. BSA protein is commonly used as model protein to determine the amount retained on the material's surface or, complementarily, the amount remaining in solution (BSA exclusion rate). Different concentrations of BSA are usually tested, and the experiment is conducted according to the desired application of the material (column, solid-phase extraction, etc.).[34,37,41]

To evaluate the proposed material and whether the amount of PEG can influence protein exclusion, the synthesized polymers were added to solutions with different concentrations of BSA and, after an interaction time, were magnetically separated and the solutions were taken for analysis. The results obtained for the protein exclusion rate for the polymers are presented in Table IV.

Table IV. Percentage of protein excluded by the materials after interaction with BSA standard solution

BSA standard solution (% m/v)	% of BSA excluded						
	MMIP	RAMIP@PEG 1	RAMIP@PEG 2	RAMIP@PEG 3	RAMIP@PEG 4	RAMIP@PEG 5	RAMIP@PEG 6
0.1	89.6	98.6	99.4	97.5	96.8	99.5	96.1
0.5	93.1	93.3	97.2	97.5	100	95.6	94.3
1.0	88.3	77.8	83.7	93.0	85.1	85.2	84.8

1: 0.025 mmol of PEG; 2: 0.0625 mmol of PEG; 3: 0.0937 mmol of PEG; 4: 0.125 mmol of PEG; 5: 0.250 mmol of PEG; 6: 0.500 mmol of PEG.

In the case of the highest concentration of standard BSA, 1.0%, for all syntheses (MMIP and all RAMIP@PEG) the polymers showed a high retention value, due the saturation of protein in solution.

Evaluating different amounts of PEG coating the RAMIP, the results obtained showed variations. Considering a balance to use the least amount of PEG possible while eliminating the highest possible concentration of protein, the most promising result was obtained for RAMIP@PEG 2, which corresponds to 0.0625 mmol of PEG. The experiment was repeated for synthesis 2 and the protein exclusion range (n = 2) was between 97.8 ± 2.2 and 96.0 ± 1.8% of excluded proteins; respectively, for concentrations of 0.1 and 0.5% of standard BSA solution. At these concentrations of BSA, MMIP presented higher percentage of retained protein, which indicates that RAMIP@PEG can successfully exclude proteins as a restricted access material. Therefore, 0.0625 mmol of PEG was adopted as optimal condition and this polymer was then analyzed and characterized by its capacity to adsorb biotin.

The proposed mechanism for protein exclusion is based on the charge density between the RAMIP@PEG surface and BSA. Under the evaluated conditions, the pH is above the isoelectric point of BSA (4.7), which has a net negative charge. The PEG layer, given its structure (Figure 1), due to the large amount of oxygen (Table II), has a negative charge density. Thus, macromolecular exclusion occurs through electrostatic repulsion.

MSPE efficiency of the polymers in biotin adsorption

To maximize biotin adsorption in RAMIP@PEG, different conditions were optimized, such as interaction time to reach equilibrium, binding solvent and adsorbent amount. All quantifications measurements were performed by HPLC.

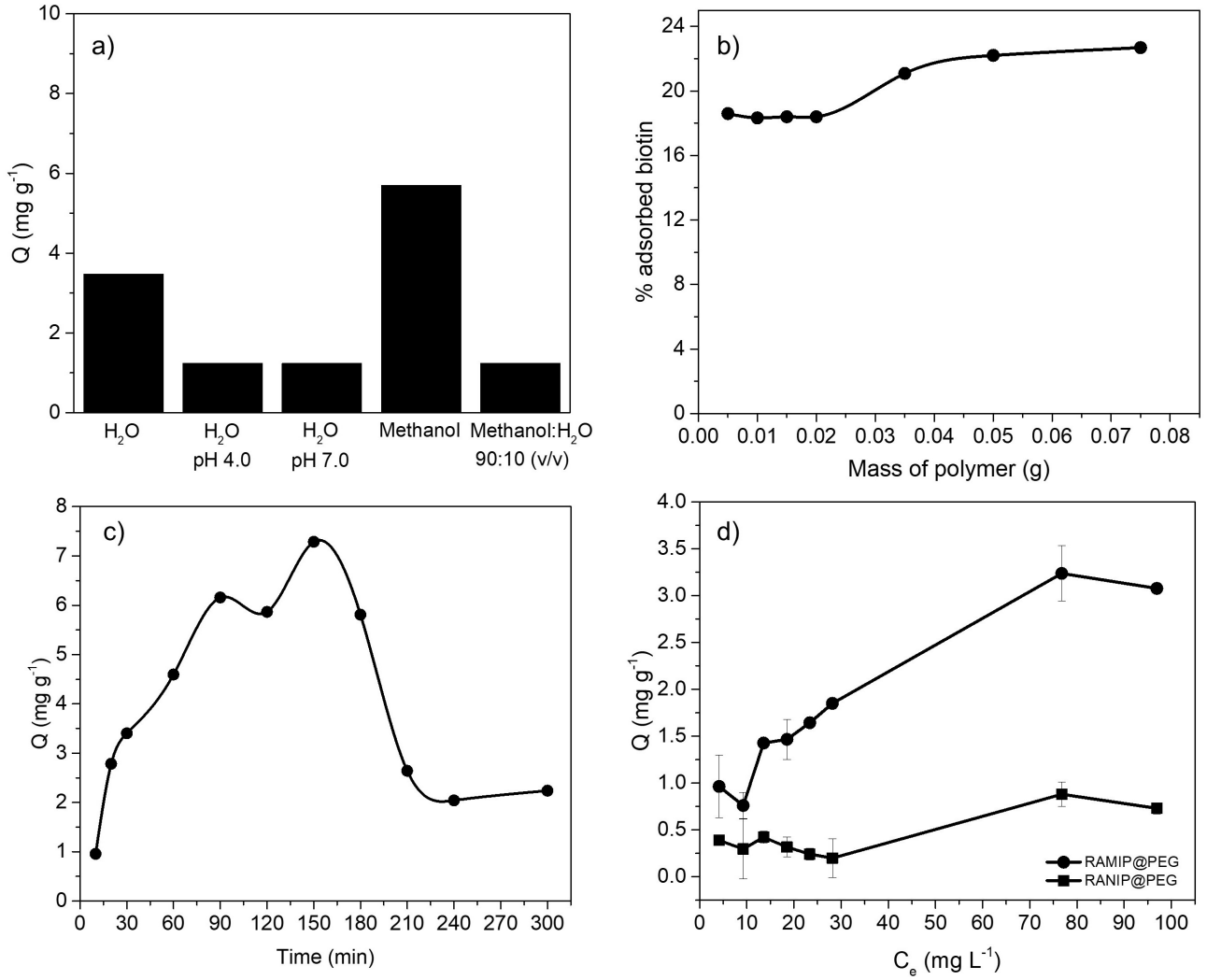

Figure 5. Optimization of biotin adsorption by RAMIP@PEG by evaluating a) effect of the binding solvent, b) amount of polymer, c) interaction time between biotin and polymer, d) adsorption isotherm for imprinted polymer and its respective control.

The first study conducted was the nature of the solvent in which biotin must be solubilized to interact with the polymer, since the medium in which the analyte is solvated directly interferes with its binding to the polymer. As shown in Figure 5a, aqueous solutions, organic solvents and mixtures in different proportions between them were evaluated, and methanol (MeOH) showed the best results, with approximately 57% retention, being the solvent adopted for subsequent studies. For aqueous solutions or mixtures between organic solvent and water, the % retention decreases. Other solutions such as ethanol, acetonitrile and mixtures were evaluated, and the polymer did not show retention, which indicates that in these cases biotin preferably remain solvated instead of binding to RAMIP@PEG.

The mass study (Figure 5b) was performed to optimize the polymer dosage, which is directly related to the extent of binding sites. The results showed that the percentage of biotin retention remained within a range without significant variations (from 18 to 23% retention) with the significant increase in RAMIP@PEG mass, possibly given by the initial concentration of analyte. Therefore, for the subsequent analyses, the polymer mass was fixed at 5.0 mg.

By optimizing the equilibrium time to provide maximum adsorption (Figure 5c), the highest biotin retention occurred between 90 and 180 min, and after 180 min, biotin desorption occurs. Since the variation in adsorption was not considerable (around 2%) in the interval between 90 and 180 min, 90 min time was chosen as the best for the analyses, as it presents the highest value of adsorbed biotin per gram of polymer (6.2 mg g^{-1}) and is not yet close to desorption occurring from 180 min onwards.

The rate of adsorption depends on the extent and the availability of adsorption sites, and the adsorption kinetics describe the rate at which the analyte is adsorbed (or desorbed) in the polymer surface, allowing to understand the process. There are four main steps in the transference mechanism of the adsorbate from a solution to the adsorbent: bulk diffusion, film (or external) diffusion, intraparticle diffusion and adsorptive attachment of the adsorbate with the surface-active sites.[42]

To evaluate the adsorption kinetics, four different models were applied in this work: pseudo-first order, pseudo-second order, intraparticle diffusion and Elovich.[42,43] Table VI shows the linear forms of the models and obtained parameters and Figure S6 the plot for each model.

Table VI. Calculated kinetic parameters from different models for biotin adsorption onto RAMIP@PEG

Model	Equation	k_1	k_2	q_e	k_{id}	C	α	β	R^2
Pseudo-first order	$\ln(q_e - q_t) = \ln q_e - k_1 t$	0.0172	–	3.93	–	–	–	–	0.60
Pseudo-second order	$\frac{t}{q_t} = \frac{1}{k_2 q_e^2} + \frac{t}{q_e}$	–	0.00233	8.48	–	–	–	–	0.91
Intraparticle diffusion	$q_t = k_{id} t^{0.5} + C$	–	–	–	0.750	0.964	–	–	0.97
Elovich	$q_t = \frac{1}{\beta}\ln(\alpha\beta) + \frac{1}{\beta}\ln t$	–	–	–	–	–	0.370	0.509	0.93

q_e = adsorption capacity at equilibrium (mg g^{-1}); q_t = amount of biotin adsorbed in each time *t* by the polymer (mg g^{-1}); t = time (minutes); k_1 = pseudo-first order rate constant (min^{-1}); k_2 = pseudo-second order rate constant (g mg^{-1} min^{-1}); k_{id} = intraparticle diffusion rate constant (mg g^{-1} $min^{-0.5}$); C = constant related to extend of thickness of the boundary layer (mg g^{-1}); β = adsorption constant (g mg^{-1}) related to surface coverage and activation energy; α = initial adsorption rate (mg g^{-1} min^{-1}).

It was not obtained a good fit to data for the pseudo-first-order model (R^2 = 0.60). This model considers that the mass transfer from the solution (external adsorption process directly proportional to the equilibrium concentration difference of the analyte in solution and on the polymer surface) is the limiting step.[42] Considering that PEG creates a barrier on the MIP surface, the mass transfer process ends up having an additional barrier to overcome, which implies that maximum adsorption occurs over longer times and a more complex mechanism over external adsorption occurs.

Pseudo-second order model presented better fit to data (R^2 = 0.91) when compared to pseudo-first order, which indicates that chemical interactions have an important role in the rate of the process and the rating limiting step of biotin onto RAMIP@PEG may be by chemisorption.[44,45] The value of rate constant (0.00233 g mg^{-1} min^{-1}) indicates a chemisorption process that is not very fast, which is consistent with what was observed in the contact time study.

The intraparticle diffusion model was employed to verify the effect of diffusion in adsorption process. If intraparticle diffusion is the rate-determining factor, the removal of the adsorbate varies with the square root of time and the plot should be a straight line passing through the origin, while the value of *C* is related to

the boundary layer thickness, that is, the greater the value of *C*, the greater the effect of the boundary layer and the surface sorption in the rate controlling step.[42,43,45] Among the four models evaluated, intraparticle diffusion presented the better fitting results to experimental data (R^2 = 0.97), with a k_{id} = 0.750 mg g^{-1} $min^{-0.5}$ and *C* = 0.964. As shown in Figure S6.c the profile can be divided in two different stages: a sharp increase followed by a plateau, and the line does not pass through the origin (value of *C* is different from zero), indicating the influence of other processes than intraparticle diffusion.

The Elovich model showed the second-best fit (R^2 = 0.93) and, although not close to 1, was the second-best model whose data fitted. This model is used to describe chemical adsorption processes on heterogeneous surfaces and the parameters obtained were = 0.370 mg g^{-1} min^{-1} and = 0.509 mg g^{-1}.

Adsorption isotherm curve of biotin in the polymers is shown in Figure 5d. The profile of adsorption indicates that the adsorption capacity of RAMIP@PEG increases with the concentration of adsorbate in equilibrium, and q_e reaches a constant value in higher concentrations of biotin. For non-imprinted polymer (RANIP@PEG) was observed a similar curve with a lower adsorption capacity, which indicates that biotin is adsorbed in selective cavities.

In order to describe the adsorption equilibrium data and understanding the mechanism of adsorption, the isotherm curve of RAMIP@PEG was correlated with different models: Langmuir, Freundlich, Elovich, Redlich-Peterson and Dubinin-Radushkevich. The Supplementary Material presents the isotherms (Figure S7) and the equations and description of each parameter for the calculated models.[42,44–47] The model fitted values based on the experimental results are shown in Table VII.

Table VII. Parameters calculated for the different adsorption isotherm models for biotin

Model	Parameter	Value
Langmuir	q_m (mg g^{-1})	4.131
	K (L mg^{-1})	0.0336
	R_L	0.856 – 0.229
	R^2	0.934
Freundlich	K (mg g^{-1})(L mg^{-1})$^{1/n}$	0.406
	1/n	0.449
	R^2	0.876
Elovich	q_m (mg g^{-1})	1.837
	K (L mg^{-1})	0.416
	R^2	0.610
Redlich-Peterson	β	0.551
	K (L g^{-1})	0.4684
	R^2	0.914
Dubinin-Radushkevich	q_m (mg g^{-1})	13.16
	K (mol^2 J^{-2})	3.87×10^{-9}
	E (kJ mol^{-1})	11.35
	R^2	0.835

Considering the models to which the adsorption isotherm data were fitted, the Langmuir model showed the best fit, with the highest coefficient of determination (R^2 = 0.934) among them. Based on this model, it is assumed that the surface of the polymers is homogeneous, with the formation of a monolayer of the analyte adsorbed at the selective sites (the active sites on the polymer surface are equivalent and energetically identical). The maximum adsorption capacity corresponds to the formation of the saturated biotin monolayer on the RAMIP@PEG surface. Considering the lowest and highest concentration values of the isotherm, the separation factor values obtained were 0.856 and 0.229, respectively; as these values are between 0 and 1, it indicates that the adsorption of the analyte on the polymer is favorable.

Other models that consider heterogeneous systems and/or multilayer adsorption, such as Freundlich, Elovich, and Dubinin-Radushkevich, presented lower R^2 values.

Restricted access MIPs exhibit different analyte adsorption and protein exclusion behaviors, which are directly related to the type of polymer structure and the restricted access strategy. Table S1 compares different types of restricted access MIPs, including their structure, reagents, and restricted access strategies. Most studies showed hydrophilic monomers and/or BSA covering as a strategy and the protein exclusion results presented by the proposed material were as efficient as, or even superior to, other reported results. Therefore, the polymer synthesized with PEG proves to be an efficient restricted access alternative while maintaining the adsorptive characteristics of the imprinted polymer.

Selectivity test

The selectivity experiment was performed to investigate the adsorption capacity of the imprinted polymer for the template as well for other molecules. The selective recognition ability of RAMIP@PEG was evaluated under separated conditions between the template (biotin) and potential interfering molecules; in this case, biocytin, NHS-SS-biotin and tetracycline. The chemical structures and analytical data for selectivity test can be observed in Figure S8 and Table VIII shows the calculated analytical parameters.

Table VIII. Distribution coefficient (K_d) and imprinting factor (*IF*) calculated from selectivity test performed with RAMIP@PEG and RANIP@PEG

Analyte	Material	K_d (L g^{-1})	*IF*
Biotin	RAMIP@PEG	0.0422	3.80
	RANIP@PEG	0.0111	
Biocytin	RAMIP@PEG	0.2192	0.96
	RANIP@PEG	0.2291	
NHS-SS-biotin	RAMIP@PEG	0.1738	0.67
	RANIP@PEG	0.2583	
Tetracycline	RAMIP@PEG	0.2251	0.88
	RANIP@PEG	0.2552	

According to Table VIII, in evaluated conditions, it can be observed that RAMIP@PEG showed retention for both biotin and its analogs, based on the obtained K_d values. In the case of biotin, the *IF* indicates that the retention occurred selectively, once the *IF* of 3.8 is significantly greater than unity, showing the formation of template-shaped cavities in RAMIP@PEG.[48]

As for the structural analogs of biotin, although they were retained by the MIP, the adsorption was non-selective, given the *IF* values obtained. This behavior is consistent with previously reported MIPs for biotin, suggesting that the cavity can accommodate the imidazole and tetrahydrothiophene rings found in both biotin and its analogs strcutures.[28] The effect of the side chain is also evident, as NHS-SS-biotin, which possesses a larger side chain, was retained to a lesser extent than biocytin.

Tetracycline was also adsorbed; given the large number of functional groups in its structure, this retention is also non-specific. However, tetracycline was selected solely due to its structural difference from biotin, and in practice it is not expected to coexist with biotin in the food samples targeted for this application.

Based on this, the use of restricted access MIPs holds significant potential for application in food quality control. Food samples are complex due to their composition (proteins, lipids, polysaccharides, etc.), and

determining water-soluble vitamins like biotin presents challenges, such as matrix effects, that can influence the response of several analytical methods. Sample pretreatment like hydrolysis technique can sometimes compromise vitamin structure; however, methods like SPE prior to instrumental analysis are effective for biotin and other water-soluble vitamins, as they allow for faster preparation while keeping the structure intact, unlike acid or alkaline hydrolysis.[49,50]

Biotin can be found in different sample matrices, such as honey, fruits, grains, meat, dairy, flour, among others, and fortified dietary supplements.[49,50] In some natural food, biotin is also present in protein-bound form as biocytin (**ε**-biotinyl-L-lysine) or biotinylated peptides.[9,10] Based on the selectivity study, the RAMIP@PEG can be successfully applied in food sample matrices due to its capacity to recognize biotin, biocytin and other biotin derivative compounds.

Thus, the use of RAMIP@PEG offers an alternative to the analytical challenges when analyzing complex food samples by eliminating the step of sample preparation. Moreover, magnetic MIPs have proven effective in MSPE applications by enabling the removal of interferents, analyte enrichment and easy separation via an external magnetic field.[20] Therefore, potential food matrices for RAMIP@PEG application includes, for example, honey and eggs.

Furthermore, the proposed material has also potential application in biomimetic assays, given that the biotinylating molecules is a procedure widely applied in analytical chemistry used for signal amplification. The use of biotin MIPs and MMIPs as substitutes for streptavidin has proven highly effective for detecting biotin and biotinylated biomolecules.[14,15] Consequently, employing restricted access MIPs would enhance analytical performance and eliminate the need for sample preparation.

CONCLUSIONS

In this work it was described the synthesis, characterization and optimization of a restricted access magnetic MIP containing polyethylene glycol as protein exclusion agent. PEG was covalently attached to the polymer surface by its functional groups and hydroxyl groups of hydrophilic monomers present in magnetic MIP surface. All materials (MMIP, RAMIP and RAMIP@PEG) were extensively characterized by several techniques; by FTIR analysis it was possible to observe the presence of hydroxyl groups in hydrophilic comonomers, and XPS measurements showed the covalently linked PEG by comparing the decrease in the number of hydroxyl groups and the increase in ester groups present from RAMIP to RAMIP@PEG. Different proportions of PEG were evaluated and RAMIP@PEG containing 0.0625 mmol of PEG presented best results in protein exclusion, with exclusion rates exceeding 96.0% under the analyzed conditions. The analytical evaluation of biotin adsorption by RAMIP@PEG, in optimal conditions, showed a maximum experimental q of approximately 3.2 mg g^{-1}, while the non-imprinted polymer (RANIP@PEG) presented lower values of adsorption, indicating that biotin bound to the selective cavities. Thus, the results obtained show that the proposed material was successfully synthesized, exhibited its restricted access property in a highly satisfactory manner, and maintained its molecular imprinting capacity by adsorbing the analyte. Selectivity assay showed that RAMIP@PEG presented adsorption capacity for biotin and biotin analogues. The use of PEG allows the imprinted polymer to be applied with restricted access in non-aqueous media and with a resistant structure to different pH values, expanding the application prospects of restricted access MIP in complex samples such as biological fluids, complexes aqueous media and food. Future prospects of the research comprehend the analytical applications of the proposed material in MSPE field to determine biotin and biotinylated compounds in different food matrices.

Acknowledgements

This study was financed, in part, by the Fundação de Amparo à Pesquisa do Estado de São Paulo (FAPESP), Brasil. Process Number #2015/04367-1.

Conflicts of interest

The authors have no conflict of interest to declare.

Declaration on the Use of Artificial Intelligence

The authors declare that no artificial intelligence tools were used in the preparation of this article.

REFERENCES

(1) Wang, P.; Zhang, L.; Liu, L.; Shen, D.; Yu, K.; Jiang, Y.; Zhou, Y.; Huang, Y.; Pan, J. How to Enhance the Recognition Activity of Molecularly Imprinted Polymer Sites: A Review. *TrAC, Trends Anal. Chem.* **2025**, *190*, 118278. https://doi.org/10.1016/j.trac.2025.118278

(2) Kalogiouri, N. P.; Kabir, A.; Furton, K. G.; Samanidou, V. F. A Tutorial on the Synthesis and Applications of Molecularly Imprinted Polymers in Analytical Chemistry. *J. Chromatogr. Open* **2025**, *8,* 100244. https://doi.org/10.1016/j.jcoa.2025.100244

(3) Sullivan, M. V.; Nanalal, S.; Dean, B. E.; Turner, N. W. Molecularly Imprinted Polymer Hydrogel Sheets with Metalloporphyrin-Incorporated Molecular Recognition Sites for Protein Capture. *Talanta* **2024**, *266,* 125083. https://doi.org/10.1016/j.talanta.2023.125083

(4) Wang, L.; Hu, J.; Wei, W.; Song, Y.; Li, Y.; Shen, Y.; Gao, G.; Qin, L. Electrochemical Paper-Based Sensor Based on Molecular Imprinted Polymer and Nitrogen-Doped Graphene for Tetracycline Determination. *Microchem. J.* **2024**, *207,* 111809. https://doi.org/10.1016/j.microc.2024.111809

(5) Singh, D.; Bhattacharya, S. Development and Evaluation of Optimized Molecularly Imprinted Polymer (MIP) for Targeted Drug Delivery of 5-Fluorouracil. *Lett. Drug Des. Discov.* **2025**, *22* (4), 100049. https://doi.org/10.1016/j.lddd.2025.100049

(6) Tian, Y.; Xu, Y.; Sun, M.; He, J.; Xie, Y. Efficient Extraction and Analysis of Carbamate Pesticides in Water Using a Solid-Phase Extraction Column Packed with Surface Molecularly Imprinted Polymers. *Microchem. J.* **2025**, *217,* 114912. https://doi.org/10.1016/j.microc.2025.114912

(7) Zhuang, S.; Li, D.; Liu, Y.; Xiong, C. Facile and Fast Fabrication of Magnetic Molecularly Imprinted Polymer for Extraction of Carbamazepine from Environmental Samples and Fish Tissues Followed by UHPLC-MS/MS Detection. *Microchem. J.* **2024**, *199,* 110063. https://doi.org/10.1016/j.microc.2024.110063

(8) van Wissen, G.; Marroquin-Garcia, R.; Frigoli, M.; Lowdon, J. W.; Cleij, T. J.; Eersels, K.; van Grinsven, B. Thermal Sensing of Syringic Acid in Food Samples via Molecularly Imprinted Polymers Synthesized from Bio-Based Deep Eutectic Solvents as Monomers. *Food Chem.* **2025**, *480,* 143947. https://doi.org/10.1016/j.foodchem.2025.143947

(9) Altun, A.; Selamioğlu, A.; Gedikbaşı, A. Biotin in Health and Disease: A Review of Its Metabolic and Pharmacological Implications. *PharmaNutrition* **2026**, *36*, 100488. https://doi.org/10.1016/j.phanu.2026.100488

(10) Karalia, S.; Meena, V. K. Biotin: DNA to Diet. *J. Nutr. Biochem.* **2025**, *146*, 110081. https://doi.org/10.1016/j.jnutbio.2025.110081

(11) Jain, A.; Cheng, K. The Principles and Applications of Avidin-Based Nanoparticles in Drug Delivery and Diagnosis. *J. Controlled Release* **2017**, *245*, 27–40. https://doi.org/10.1016/j.jconrel.2016.11.016

(12) Bayer, E. A.; Wilchek, M. Application of Avidin-Biotin Technology to Affinity-Based Separations. *J. Chromatogr.* **1990**, *510*, 3–11. https://doi.org/10.1016/S0021-9673(01)93733-1

(13) Wilchek, M.; Bayer, E. A. Introduction to Avidin-Biotin Technology. *Methods Enzymol.* **1990**, *184*, 5–13. https://doi.org/10.1016/0076-6879(90)84256-G

(14) Marfà, J.; del Valle, A.; Pupin, R. R.; Baro, B.; Bassat, Q.; Sotomayor, M. D. P. T.; Pividori, M. I. Biotin-Specific Molecularly Imprinted Polymers as a Biomimetic Test Line in Lateral Flow Assays. *Biosens. Bioelectron.* **2026**, *298*, 118415. https://doi.org/10.1016/j.bios.2026.118415

(15) Ben Aissa, A.; Herrera-Chacon, A.; Pupin, R. R.; Sotomayor, M. D. P. T.; Pividori, M. I. Magnetic Molecularly Imprinted Polymer for the Isolation and Detection of Biotin and Biotinylated Biomolecules. *Biosens. Bioelectron.* **2017**, *88*, 101–108. https://doi.org/10.1016/j.bios.2016.07.096

(16) Liu, Y.; Wang, L.; Li, H.; Zhao, L.; Ma, Y.; Zhang, Y.; Liu, J.; Wei, Y. Rigorous Recognition Mode Analysis of Molecularly Imprinted Polymers—Rational Design, Challenges, and Opportunities. *Prog. Polym. Sci.* **2024**, *150*, 101790. https://doi.org/10.1016/j.progpolymsci.2024.101790

(17) Lamaoui, A.; Mani, V.; Durmus, C.; Salama, K. N.; Amine, A. Molecularly Imprinted Polymers: A Closer Look at the Template Removal and Analyte Binding. *Biosens. Bioelectron.* **2024**, *243*, 115774. https://doi.org/10.1016/j.bios.2023.115774
(18) Dikici, E.; Ay, D.; Gök, T.; Karakoç, V.; İnanan, T.; Acet, B. Ö.; Odabaşı, M.; Acet, Ö. The Rise of Molecularly Imprinted Polymers in Food Analysis: Selective, Reliable, and Cost-Effective Approaches. *Food Chem.* **2025**, *497*, 146960. https://doi.org/10.1016/j.foodchem.2025.146960
(19) Martins, R. O.; Batista Junior, A. C.; Brito, C. C. S. M.; Rocha, Y. A.; Chaves, A. R. Molecularly Imprinted Polymers in Solid-Phase Microextraction: Enhancing the Analysis of Pharmaceutical Compounds across Diverse Sample Matrices. *Journal of Pharmaceutical and Biomedical Analysis Open* **2024**, *4*, 100037. https://doi.org/10.1016/j.jpbao.2024.100037
(20) Wang, H.; Huang, C.; Ma, S.; Bo, C.; Ou, J.; Gong, B. Recent Advances of Restricted Access Molecularly Imprinted Materials and Their Applications in Food and Biological Samples Analysis. *TrAC, Trends Anal. Chem.* **2022**, *147*, 116526. https://doi.org/10.1016/j.trac.2022.116526
(21) Torabi, E.; Abdar, A.; Lotfian, N.; Bazargan, M.; Simms, C.; Moussawi, M. A.; Amiri, A.; Mirzaei, M.; Parac-Vogt, T. N. Advanced Materials in Sorbent-Based Analytical Sample Preparation. *Coord. Chem. Rev.* **2024**, *506*, 215680. https://doi.org/10.1016/j.ccr.2024.215680
(22) Mendes, T.; Rosa, M.; Figueiredo, E. Restricted Access Molecularly Imprinted Polymers for Biological Sample Preparation. *Braz. J. Anal. Chem.* **2021**, *9* (35), 18-38. https://doi.org/10.30744/brjac.2179-3425.RV-90-2021
(23) Mendes, T. V.; Franqui, L. S.; Santos, M. G.; Wisniewski, C.; Figueiredo, E. C. Synthesis and Characterization of a New Magnetic Restricted Access Molecularly Imprinted Polymer for Biological Sample Preparation. *Mater. Today Commun.* **2020**, *24, 101002*. https://doi.org/10.1016/j.mtcomm.2020.101002
(24) Shi, L.; Zhang, J.; Zhao, M.; Tang, S.; Cheng, X.; Zhang, W.; Li, W.; Liu, X.; Peng, H.; Wang, Q. Effects of Polyethylene Glycol on the Surface of Nanoparticles for Targeted Drug Delivery. *Nanoscale* **2021**, *13* (24), 10748–10764. https://doi.org/10.1039/D1NR02065J
(25) Luan, J.; Liu, K. K.; Tadepalli, S.; Jiang, Q.; Morrissey, J. J.; Kharasch, E. D.; Singamaneni, S. PEGylated Artificial Antibodies: Plasmonic Biosensors with Improved Selectivity. *ACS Appl. Mater. Interfaces* **2016**, *8* (36), 23509–23516. https://doi.org/10.1021/acsami.6b07252
(26) Zhang, R.; Sun, Z.; Zhu, C.; Zhao, M. Dopamine-Based Molecularly Imprinted Polymers: Synthesis Strategies, Biomedical Applications, and Future Perspectives. *TrAC, Trends Anal. Chem.* **2025**, *193*, 118481. https://doi.org/10.1016/j.trac.2025.118481
(27) Pupin, R. R.; Foguel, M. V.; Gonçalves, L. M.; Sotomayor, M. del P. T. Magnetic Molecularly Imprinted Polymers Obtained by Photopolymerization for Selective Recognition of Penicillin G. *J. Appl. Polym. Sci.* **2020**, *137* (13), 48496. https://doi.org/10.1002/app.48496
(28) Uzuriaga-Sánchez, R. J.; Khan, S.; Wong, A.; Picasso, G.; Pividori, M. I.; Sotomayor, M. D. P. T. Magnetically Separable Polymer (Mag-MIP) for Selective Analysis of Biotin in Food Samples. *Food Chem.* **2016**, *190*, 460–467. https://doi.org/10.1016/j.foodchem.2015.05.129
(29) Hosangadi, B. D.; Dave, R. H. An Efficient General Method for Esterification of Aromatic Carboxylic Acids. *Tetrahedron Lett.* **1996**, *37* (35), 6375–6378. https://doi.org/10.1016/0040-4039(96)01351-2
(30) Adauto, A.; Morante, G.; Fermin, B.; Tuesta, J. C.; Khan, S.; Vega-Chacón, J.; Sotomayor, M. D. P. T.; López, R.; Picasso, G. Fabrication and Analysis of a Molecularly Imprinted Polymer (MIP) for Ivermectin: Theoretical Modeling, Synthesis, Characterization and Adsorption Evaluation. *Polym. Bull.* **2026**, *83*, 528. https://doi.org/10.1007/s00289-026-06589-x
(31) de Faria, H. D.; Abrão, L. C. de C.; Santos, M. G.; Barbosa, A. F.; Figueiredo, E. C. New Advances in Restricted Access Materials for Sample Preparation: A Review. *Anal. Chim. Acta* **2017**, *959*, 43–65. https://doi.org/10.1016/j.aca.2016.12.047
(32) Bompart, M.; Haupt, K. Molecularly Imprinted Polymers and Controlled/Living Radical Polymerization. *Aust. J. Chem.* **2009**, *62* (8), 751–761. https://doi.org/10.1071/CH09124

(33) Santos, M. G.; Moraes, G. de O. I.; Nakamura, M. G.; dos Santos-Neto, Á. J.; Figueiredo, E. C. Restricted Access Molecularly Imprinted Polymers Obtained by Bovine Serum Albumin and/or Hydrophilic Monomers' External Layers: A Comparison Related to Physical and Chemical Properties. *Analyst* **2015**, *140* (22), 7768–7775. https://doi.org/10.1039/C5AN01482D

(34) Mendes, T. V.; Franqui, L. S.; Santos, M. G.; Wisniewski, C.; Figueiredo, E. C. Synthesis and Characterization of a New Magnetic Restricted Access Molecularly Imprinted Polymer for Biological Sample Preparation. *Mater. Today Commun.* **2020**, *24*, 101002. https://doi.org/10.1016/j.mtcomm.2020.101002

(35) Chen, Y.; Zheng, R.; Cheng, Z.; Liu, Y.; Qi, G.; Chen, G. A Surface Molecularly Imprinted Magnetic Material for Rapid Recognition and Detection of Sulfonamides in Animal-Derived Foods. *Microchem. J.* **2026**, *224,* 117886. https://doi.org/10.1016/j.microc.2026.117886

(36) Huang, H.; Wen, G.; Liang, A.; Jiang, Z. A New SERS Quantitative Analysis Strategy for Ultratrace Chloramphenicol with Fe_3O_4@MIP Nanocatalytic Probe. *Spectrochim. Acta A Mol. Biomol. Spectrosc.* **2024**, *322,* 124732. https://doi.org/10.1016/j.saa.2024.124732

(37) Vidal, D. F.; Pires, B. C.; Borges, M. M. C.; de Oliveira, H. L.; Silva, C. F.; Borges, K. B. Magnetic Solid-Phase Extraction Based on Restricted-Access Molecularly Imprinted Polymers for Ultrarapid Determination of Ractopamine Residues from Food Samples by Capillary Electrophoresis. *J. Chromatogr. A* **2024**, *1720*, 464809. https://doi.org/10.1016/j.chroma.2024.464809

(38) de Paula, D. D. M.; da Silva, R. C. S.; Dinali, L. A. F.; Silva, C. F.; de Oliveira, M. A. L.; Pereira, A. C.; Borges, K. B. Magnetic Solid Phase Extraction Based on Restricted Access Molecularly Imprinted Polymer with Dually Coated for Enantioselective Determination of Tramadol in Human Plasma by Capillary Electrophoresis with Ultraviolet Detection. *Talanta* **2025**, *288*, 127676. https://doi.org/10.1016/j.talanta.2025.127676

(39) de Oliveira, H. L.; Pires, B. C.; Teixeira, L. S.; Dinali, L. A. F.; Simões, N. S.; Borges, W. de S.; Borges, K. B. Novel Restricted Access Material Combined to Molecularly Imprinted Polymer for Selective Magnetic Solid-Phase Extraction of Estrogens from Human Urine. *Microchem. J.* **2019**, *149*, 104043. https://doi.org/10.1016/j.microc.2019.104043

(40) Thommes, M.; Kaneko, K.; Neimark, A. V.; Olivier, J. P.; Rodriguez-Reinoso, F.; Rouquerol, J.; Sing, K. S. W. Physisorption of Gases, with Special Reference to the Evaluation of Surface Area and Pore Size Distribution (IUPAC Technical Report). *Pure Appl. Chem.* **2015**, *87* (9–10), 1051–1069. https://doi.org/10.1515/pac-2014-1117

(41) Cai, T.; Zhou, Y.; Liu, H.; Li, J.; Wang, X.; Zhao, S.; Gong, B. Preparation of Monodisperse, Restricted-Access, Media-Molecularly Imprinted Polymers Using Bi-Functional Monomers for Solid-Phase Extraction of Sarafloxacin from Complex Samples. *J. Chromatogr. A* **2021**, *1642*, 462009. https://doi.org/10.1016/j.chroma.2021.462009

(42) Nizam, T.; Krishnan, K. A.; Joseph, A.; Krishnan, R. R. Isotherm, Kinetic and Thermodynamic Modelling of Liquid Phase Adsorption of the Heavy Metal Ions Zn(II), Pb(II) and Cr(VI) onto $MgFe_2O_4$ Nanoparticles. *Groundw. Sustain. Dev.* **2024**, *25*, 101120. https://doi.org/10.1016/j.gsd.2024.101120

(43) Pupin, R. R.; Sotomayor, M. D. P. T. Synthesis and Evaluation of Hollow Porous Molecularly Imprinted Polymer for Selective Determination of Tetracycline. *J. Mater. Sci.* **2022**, *57* (36), 17291–17303. https://doi.org/10.1007/s10853-022-07727-2

(44) Kurczewska, J.; Cegłowski, M. Alginate vs Chitosan Composites Loaded with Halloysite/Molecularly Imprinted Polymer Hybrids for Tetracycline Removal: Comparative Studies of Adsorption Behaviour. *Int. J. Biol. Macromol.* **2025**, *307*, 142000. https://doi.org/10.1016/j.ijbiomac.2025.142000

(45) Kaveeshwar, A. R.; Ponnusamy, S. K.; Revellame, E. D.; Gang, D. D.; Zappi, M. E.; Subramaniam, R. Pecan Shell Based Activated Carbon for Removal of Iron(II) from Fracking Wastewater: Adsorption Kinetics, Isotherm and Thermodynamic Studies. *Process and Environmental Protection* **2018**, *114*, 107–122. https://doi.org/10.1016/j.psep.2017.12.007

(46) Adauto, A.; Khan, S.; Vega-Chacón, J.; Sotomayor, M. D. P. T.; Picasso, G. Effect of Functional Monomers on the Binding Properties of Molecularly Imprinted Polymers (MIPs) for Selective Recognition of Dexamethasone. *Polym. Eng. Sci.* **2025**, *65* (4), 1716–1732. https://doi.org/10.1002/pen.27082
(47) Kalam, S.; Abu-Khamsin, S. A.; Kamal, M. S.; Patil, S. Surfactant Adsorption Isotherms: A Review. *ACS Omega* **2021**, *6* (48), 32342–32348. https://doi.org/10.1021/acsomega.1c04661
(48) Barzallo, D.; Palacio, E.; Ferrer, L.; Sotomayor, M. del P. T. All-in-One Spot Test Method for Tetracycline Using Molecularly Imprinted Polymer-Coated Paper Integrated into a Portable 3D Printed Platform with Smartphone-Based Fluorescent Detection. *Talanta* **2025**, *281,* 126856. https://doi.org/10.1016/j.talanta.2024.126856
(49) Tikeshwari; Shrivas, K.; Tandey, K.; Sharma, A.; Chandrawanshi, N. K.; Ghosh, K. K. Advances and Challenges in Sample Preparation and Analytical Methods for Water-Soluble Vitamins: Application in Food, Clinical, Pharmaceutical Samples. *J. Pharm. Biomed. Anal.* **2025**, *266*, 117124. https://doi.org/10.1016/j.jpba.2025.117124
(50) Barbayanov, K.; Vovk, M.; Bulatov, A.; Timofeeva, I. Liquid-Liquid Microextraction Based on in Situ Decomposition of Deep Eutectic Solvent and Following Formation of Supramolecular Solvent: Determination of Biotin in Food Samples. *J. Food Compos. Anal* **2025**, *146*, 107910. https://doi.org/10.1016/j.jfca.2025.107910

SUPPLEMENTARY MATERIAL

Rebidding experiments in RAMIP@PEG optimization (Equation S1)

$$\%\ of\ adsorbed\ biotin = \frac{C_i - C_e}{C_i} \times 100 \qquad \text{(S1)}$$

where C_i is the initial and C_e is the equilibrium concentration of biotin in solution (in mg L^{-1}).

Synthesis of the materials

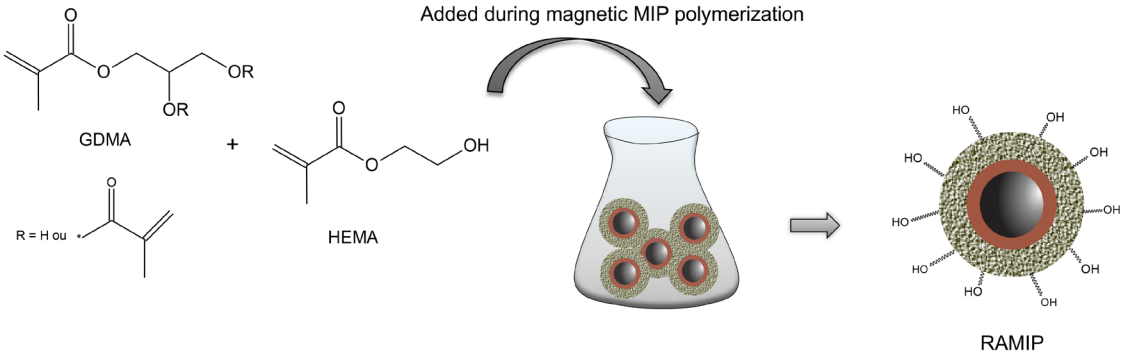

Figure S1. Proposed synthesis scheme of RAMIP obtention by adding hydrophilic comonomers HEMA and GDMA after 45 min of polymerization (RAMIP 2).

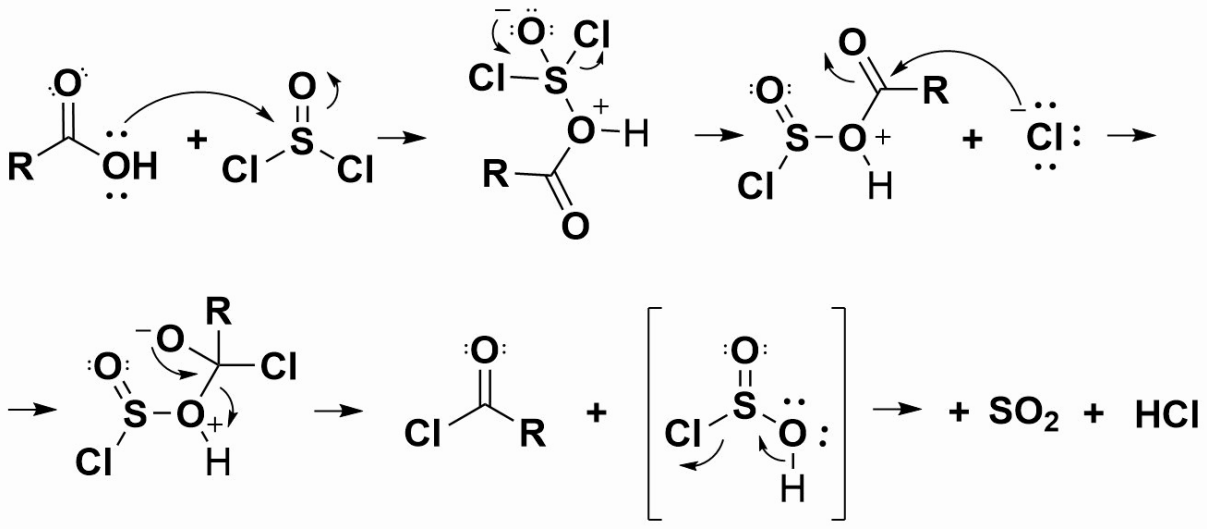

Figure S2. Mechanism of formation of the chlorinated derivative of PEG.

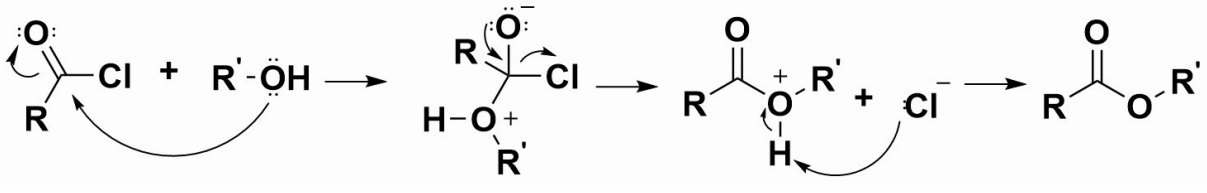

Figure S3. Mechanism of the esterification reaction between the hydroxyl group of RAMIP and the chlorinated derivative of PEG.

Characterizations

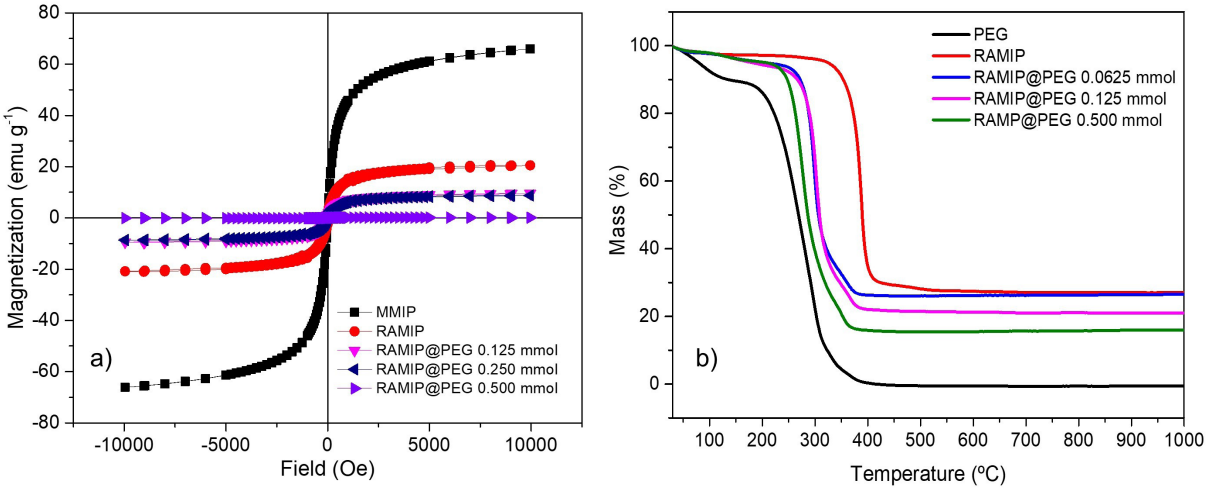

Figure S4. a) Saturation magnetization values for each synthesized material, including different proportions of PEG in each synthesis; b) TG curves for stability analysis of the polymers.

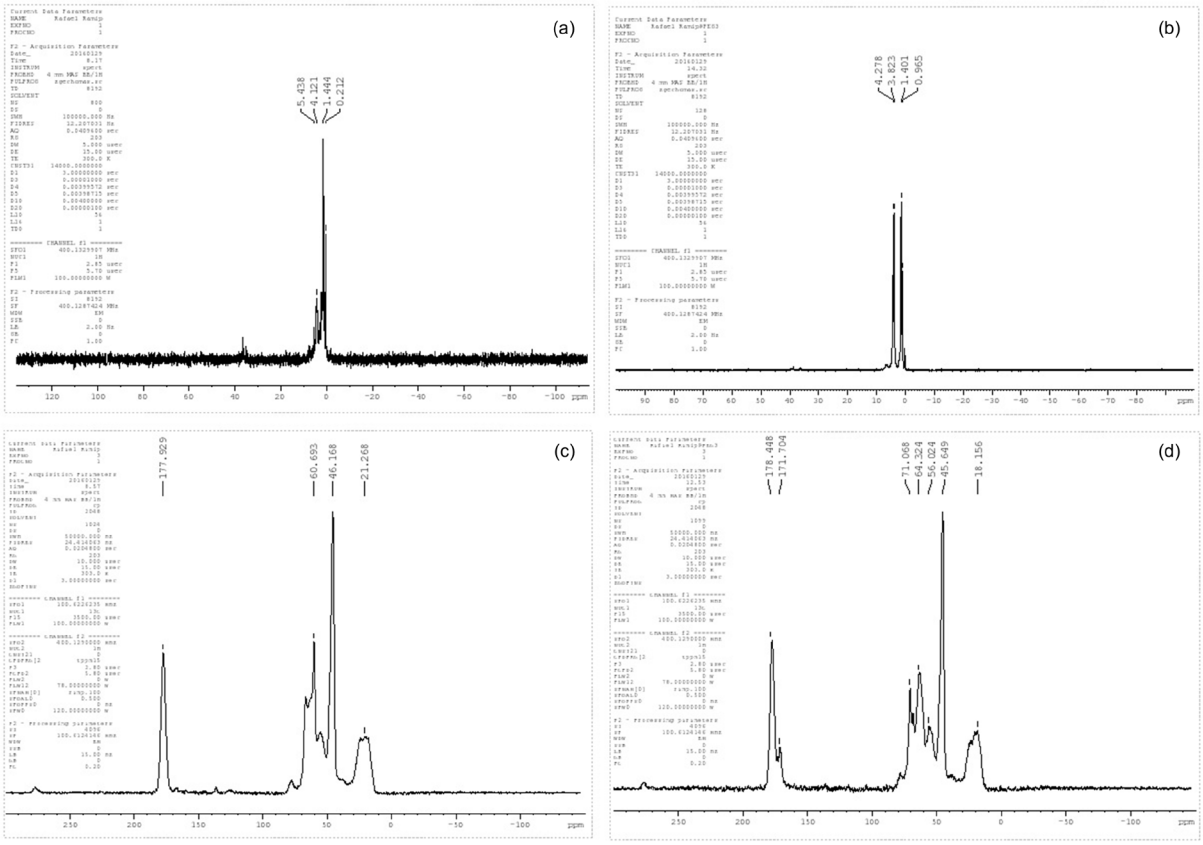

Figure S5. Solid-state ^{1}H NMR spectra of a) RAMIP, b) RAMIP@PEG and solid state ^{13}C NMR spectra of c) RAMIP and d) RAMIP@PEG (400 MHz).

Adsorption kinetic models

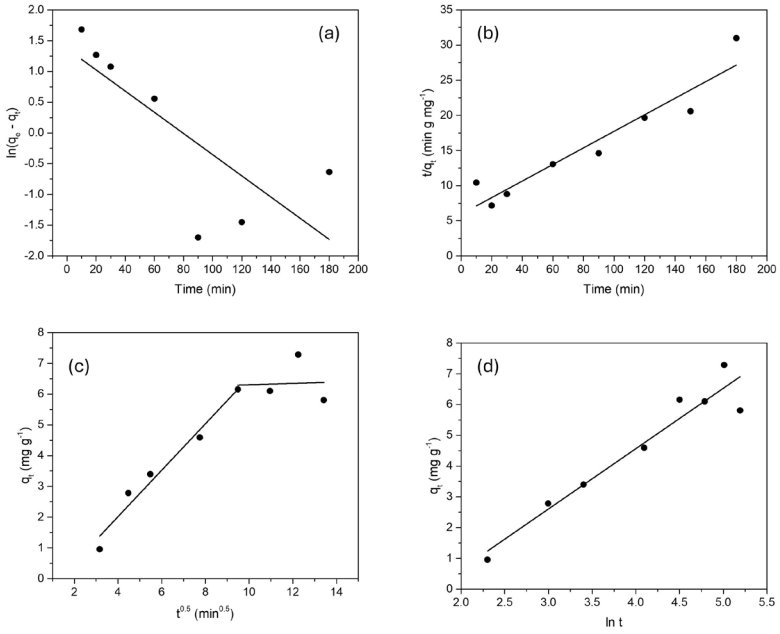

Figure S6. a) Pseudo-first order, b) Pseudo-second order, c) Intraparticle diffusion and d) Elovich kinetic model for the adsorption of biotin onto RAMIP@PEG.

Adsorption isotherm models

Langmuir model

The linear form of Langmuir equation is expressed as Equation S2:

$$\frac{C_e}{q_e} = \frac{1}{q_m K_L} + \frac{C_e}{q_m} \quad \text{(S2)}$$

where q_m (mg g^{-1}) is the maximum adsorption capacity of biotin by the polymer, K_L (L mg^{-1}) is the Langmuir constant related to the affinity of the binding sites.

Separation factor (R_L) is a dimensionless constant that expresses the affinity between adsorbate and adsorbent, indicating the nature of adsorption (Equation S3):

$$R_L = \frac{1}{1 + C_0 K_L} \quad \text{(S3)}$$

where C_o is the initial concentration of biotin (mg L^{-1}). When R_L = 0 the adsorption is irreversible, if 0 < R_L < 1 the adsorption is favorable, when R_L = 1 adsorption is linear and if R_L > 1 adsorption is unfavorable.

Freundlich model

Freundlich isotherm equation in linear form is given as Equation S4:

$$log q_e = \frac{1}{n} log C_e + \log K_F \quad \text{(S4)}$$

where K_F (mg g^{-1} (L mg^{-1})$^{1/n}$) is the maximum adsorption capacity at equilibrium concentration of biotin and $1/n$ is the heterogeneity factor and describes the strength of adsorption and the favorability of the adsorption process. For $n \geq 1$ adsorption process is favorable and for $n < 1$ the process is less favorable. The value of $1/n$ closer or equal to 1 indicates homogenous adsorption sites, while $1/n$ value closer to zero indicates a heterogeneous site.

Elovich model

Elovich linear equation is expressed as Equation S5:

$$ln \frac{q_e}{C_e} = \ln K_E q_m - \frac{q_e}{q_m} \quad \text{(S5)}$$

where K_E (L mg^{-1}) is the Elovich constant related to the maximum affinity at equilibrium and q_m (mg g^{-1}) is the monolayer maximum adsorption capacity of the adsorbent.

Redlich-Peterson model

The Redlich-Peterson model is a combination of Freundlich and Langmuir isotherms. The linear form of Redlich-Peterson isotherm can be expressed as Equation S6:

$$\ln \frac{C_e}{q_e} = \beta \ln C_e - \ln K_{RP} \quad \text{(S6)}$$

where β is and exponent in the range between 0 and 1 (when β values tending to 1, in low concentrations, the model approaches Langmuir and when β value tends to 0, Redlich-Peterson model approaches Freundlich model) and K_{RP} is the Redlich-Peterson constant (L g^{-1}).

Dubinin-Radushkevich model

The linearized form of Dubinin-Radushkevich equation is given as Equation S7:

$$\ln q_e = lnq_m - K_{DR}\varepsilon^2 \qquad \text{(S7)}$$

where q_m (mg g^{-1}) is the maximum adsorption capacity of the polymer, K_{DR} is the activity coefficient related to adsorption energy ($mol^2\ J^{-2}$) and ε is the Polanyi potential related to the equilibrium concentration. These parameters are related as Equation S8:

$$\varepsilon = RT \ln\left(1 + \frac{1}{C_e}\right) \qquad \text{(S8)}$$

The free energy E (kJ mol^{-1}), based on this model, can be calculated as Equation S9:

$$E = \frac{1}{\sqrt{K_{DR}}} \qquad \text{(S9)}$$

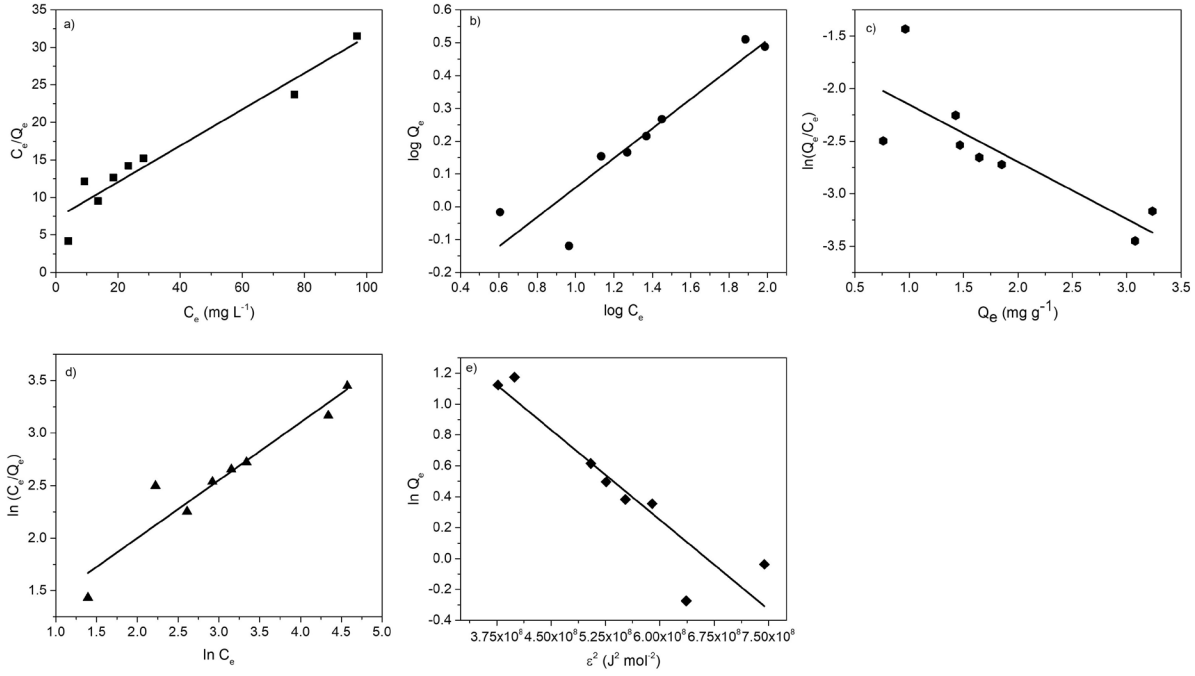

Figure S7. Models of biotin adsorption isotherms by RAMIP@PEG: a) Langmuir, b) Freundlich, c) Elovich, d) Redlich-Peterson and e) Dubinin-Radushkevich.

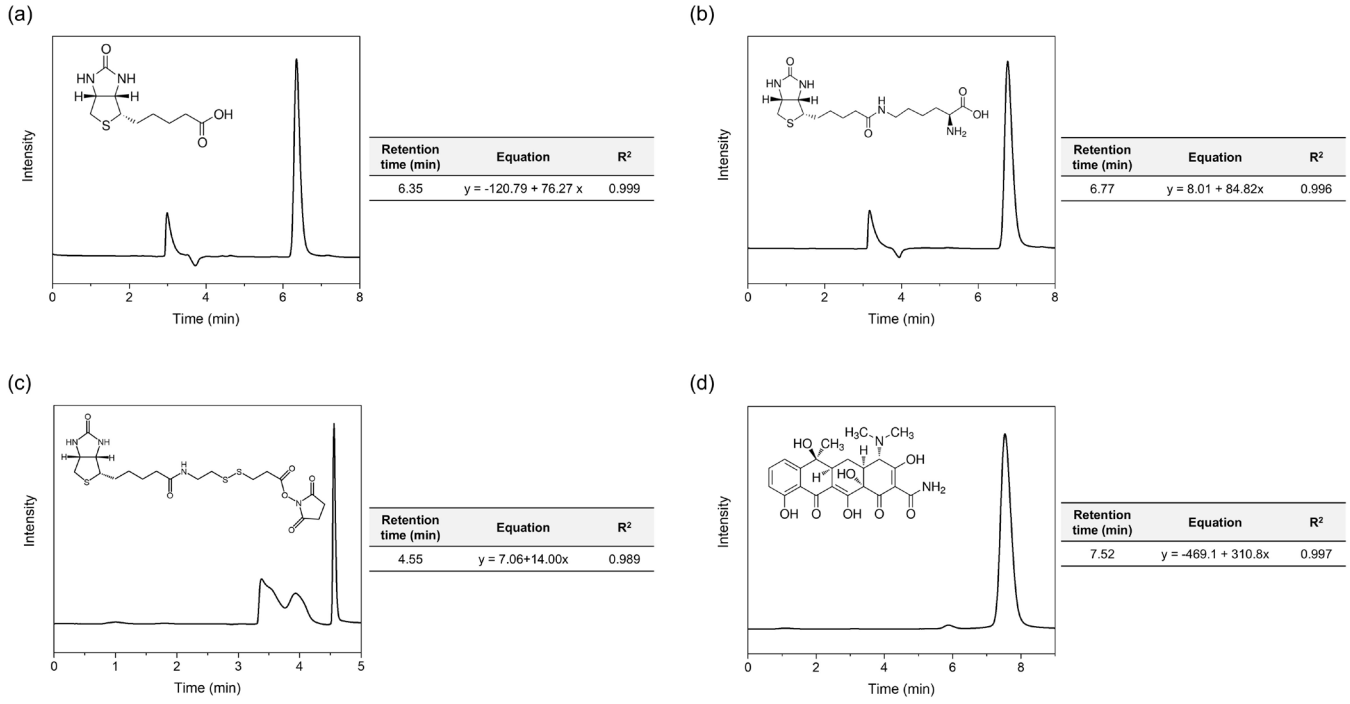

Retention time (min)	Equation	R^2
6.35	y = -120.79 + 76.27 x	0.999

Retention time (min)	Equation	R^2
6.77	y = 8.01 + 84.82x	0.996

Retention time (min)	Equation	R^2
4.55	y = 7.06+14.00x	0.989

Retention time (min)	Equation	R^2
7.52	y = -469.1 + 310.8x	0.997

Figure S8. Chemical structure, model chromatogram (80 mg L^{-1} in methanol solution) and analytical parameters for each compound evaluated in the selectivity test: a) biotin, b) biocytin, c) NHS-SS-biotin, and d) tetracycline. All substances were quantified by HPLC.

Table S1. Evaluation of restricted access molecularly imprinted polymers and its characteristics

Analyte	Sample	Detection	Material structure	Material application	Hydrophilic monomers (HM)	Restricted access strategy	Protein exclusion capacity	Ref.
Tramadol	Human plasma	Capillary electrophoresis	Core-shell	MSPE	HEMA, GDMA	HM and BSA covering	BSA covering: 91.51%; HM: 86.42%	38
Tetracycline	Milk	Fluorescence	Core-shell	MSPE	zwitterionic 2-methacryloyloxyethyl phosphorylcholine	zwitterionic polymer grafting	> 96.8%	S1
Mebendazole Albendazole	Milk	ESI-MS/MS	Polymer particles	Online SPE	GMA[a]	BSA covering	HM: 79.6% for casein; BSA covering: 93.4% for casein and 98.9% for BSA	S2
Ractopamine	Bovine milk, bovine and porcine muscle	Capillary electrophoresis	Core-shell	MSPE	HEMA, GDMA	BSA covering	91.3%	37
Phthalates[b]	Bottled water, juice and milk	GC-MS	Core-shell	MSPE	3-GPTMS[a]	HM	–	S3
Bile acids	Human serum	LC-MS	Spherical polymers particles	Online SPE	HEMA, GDMA	BSA covering	99%	S4
Sarafloxacin	Egg	HPLC	Core-shell	SPE	GMA	HM grafting	97.4%	41
Biotin[c]	–	HPLC	Core-shell MIP	MSPE	HEMA, GDMA	PEG covering	96.0-97.8%	This work

3-GPTMS: (3-glycidyloxypropyl)trimethoxysilane; BSA: bovine serum albumin; ESI-MS/MS: electrospray ionization-tandem mass spectrometry; GC-MS: gas chromatography-mass spectrometry; GDMA: glycerol dimethacrylate; GMA: glycidyl methacrylate; HEMA: 2-hydroxyethyl methacrylate; HM: hydrophilic monomers; HPLC: high performance liquid chromatography; LC-MS: liquid chromatography-mass spectrometry; MIP: molecularly imprinted polymer; MSPE: magnetic solid phase extraction; PEG: polyethylene glycol.

[a] These comonomers became hydrophilic after a chemical reaction (in acidic medium) to open the epoxide ring of its structure.
[b] The work focuses on analytical determination of several phthalates structures.
[c] The work focuses on the synthesis and characterization of the proposed material.

SUPPLEMENTARY REFERENCES

(S1) Li, Y.; Zhao, W.; Tang, X.; Xu, F.; Bo, C. Magnetic Molecular Imprinting-Restricted Access Materials Combined with Luminous Boric Acid Carbon Dots for Fluorescence Monitoring of Tetracycline. *Microchem. J.* **2025**, *214*, 113966. https://doi.org/10.1016/j.microc.2025.113966

(S2) Lourêdo, A. A. M.; Pereira, H. H.; Bonfilio, R.; Santos, M. G. Online Restricted Access Molecularly Imprinted Solid Phase Extraction Coupled with Electrospray Ionization-Tandem Mass Spectrometry for Determination of Mebendazole and Albendazole in Milk Samples. *J. Chromatogr. A* **2024**, *1737*, 465466. https://doi.org/10.1016/j.chroma.2024.465466

(S3) Bhogal, S.; Mohiuddin, I.; Kim, K.-H.; Malik, A. K.; Kaur, K. Restricted Access Medium Magnetic Molecularly Imprinted Polymers: Validation of Their Suitability as an Effective Quantitation Tool against Phthalates in Food Products Packaged in Plastic. *Chem. Eng. J.* **2023**, *457*, 141270. https://doi.org/10.1016/j.cej.2023.141270

(S4) Silveira, A. T.; Barbosa, A. M. da C.; de Faria, H. D.; Marciano, L. P. de A.; Figueiredo, E. C.; Martins, I. Online Restricted Access Molecularly Imprinted Solid-Phase Extraction Coupled with Liquid Chromatography-Mass Spectrometry for the Selective Determination of Serum Bile Acids. *Analyst* **2022**, *147* (12), 2779-2792. https://doi.org/10.1039/d2an00446a